AD-A052 227 RHODE ISLAND UNIV KINGSTON DEPT OF ELECTRICAL ENGIN--ETC F/G 20/1
UNDERWATER SURFACE WAVE PROPAGATION, AND ASSOCIATED RADIATION.(U)
JUN 63 M P FEDER, F H MIDDLETON NONR-396(12)
UNCLASSIFIED TR-2 NL

| OF |
AD A052227


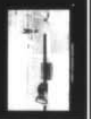




END
DATE FILMED
5-78
DDC

DIVISION OF ENGINEERING RESEARCH AND DEVELOPMENT

DEPARTMENT OF ELECTRICAL ENGINEERING

(1)
BS

Underwater Surface Wave Propagation, and Associated Radiation

by M. P. FEDER and F. H. MIDDLETON

Contract No. Nonr-396(12)
Technical Report No. 2

Prepared for
ACOUSTICS PROGRAMS
Naval Applications Group
Office of Naval Research

UNIVERSITY OF RHODE ISLAND
KINGSTON, RHODE ISLAND

University of Rhode Island
Division of Engineering Research and Development
Electrical Engineering Department

(9) Technical rept,

Technical Report No. 2

(14) TR-2

(6)

UNDERWATER SURFACE WAVE PROPAGATION, AND ASSOCIATED RADIATION

by

(10) M. P. Feder
Research Assistant
and
F. H. Middleton
Professor

(12) 60 p.

(11) 16 Jun 63

Sponsor: Office of Naval Research
Acoustics Programs, Code 468
(15) Washington 25, D.C.
Contract: Nonr-396(12)
Date: June 16, 1963

I. INTRODUCTION

The surface waves of Rayleigh were first studied in detail in seismology where they represent a principal part of an elastic wave coming from distant earth tremors. During the last 10-15 years they have acquired considerable significance in ultrasonics for flaw detection and for locating surface defects.

These surface waves are "attached" to the boundary between two media, one of which must be an elastic solid, and are confined to a region near the surface, giving little movement at great depth. These are important at great distances from the point of origin for the following reason. A pulse traveling symmetrically outwards from a point source in three dimensions gives a displacement inversely proportional to the distance r from the source. But if the disturbance is confined to a given depth h, (cylindrical symmetry) its energy over a band at a distance r is distributed over an area $2\pi rh$ and therefore the amplitude of the disturbance will vary as $r^{-1/2}$. At large distances the surface wave may predominate over other types of waves, and this actually occurs in the case of earthquakes.

An interesting application of surface waves is in the field of underwater acoustic wave launchers and receivers. Electromagnetic surface wave antennas are now used in radio communications and a somewhat analogous arrangement may be possible in sonar work. Present day acoustic antennas

depend upon (excepting linear arrays) their cross sectional dimension to control the beam pattern. To obtain a narrow pattern a large cross section (in terms of wavelength) is necessary. However, large frontal areas are hydrodynamically incompatible with high speed underwater vehicles. In a surface wave antenna the length of the radiator rather than the cross section is of primary importance in the production of a large directivity index. But before any worthwhile radiator can be designed, information concerning the transmission of surface wave energy between media must be available.

This paper deals with this question of surface wave transmission specializing in the field of launching underwater acoustic energy. Included will be a discussion of the mathematics of surface waves associated with boundaries between a solid and a vacuum, and a solid and a liquid. A description is given of the experimental setup and the resulting beam patterns obtained from surface waves launched from metallic rectangular bars will be shown.

II. WAVES IN ELASTIC MATERIAL

Before any understanding can be achieved as to the nature of surface waves a general understanding of the mathematics of waves in elastic bodies is a necessity. A classic reference is the Theory of Elasticity by S. Timoshenko.[1] A brief review of waves in elastic materials will now be undertaken.

Assume an isotropic cube of elastic solid as shown in Figure 1 on the following page. Summing the forces in any one direction, for instance the x direction, we obtain

$$\Sigma F_x = \left(\sigma_x + \frac{\partial \sigma_x}{\partial x}\ \delta_x\right)\delta_y\delta_z - \sigma_x\delta_y\delta_z + \left(\tau_{xy} + \frac{6\tau_{xy}}{\partial y}\ \delta_y\right)\delta_x\delta_z$$

$$- \tau_{xy}\delta_x\delta_z + \left(\tau_{xz} + \frac{\partial \tau_{xz}}{\partial z}\ \delta_x\delta_y - \tau_{xz}\delta_x\delta_y \right. \qquad (1)$$

$$+ X\delta_x\delta_y\delta_z = 0$$

where σ_x = Normal stress parallel to x axis

τ_{ij} = Stress on j face parallel to i axis

X = Component of body force per unit volume in x direction

$\delta_x, \delta_y, \delta_z$ = Sides of the cube

Superscripts refer to references listed in the bibliography

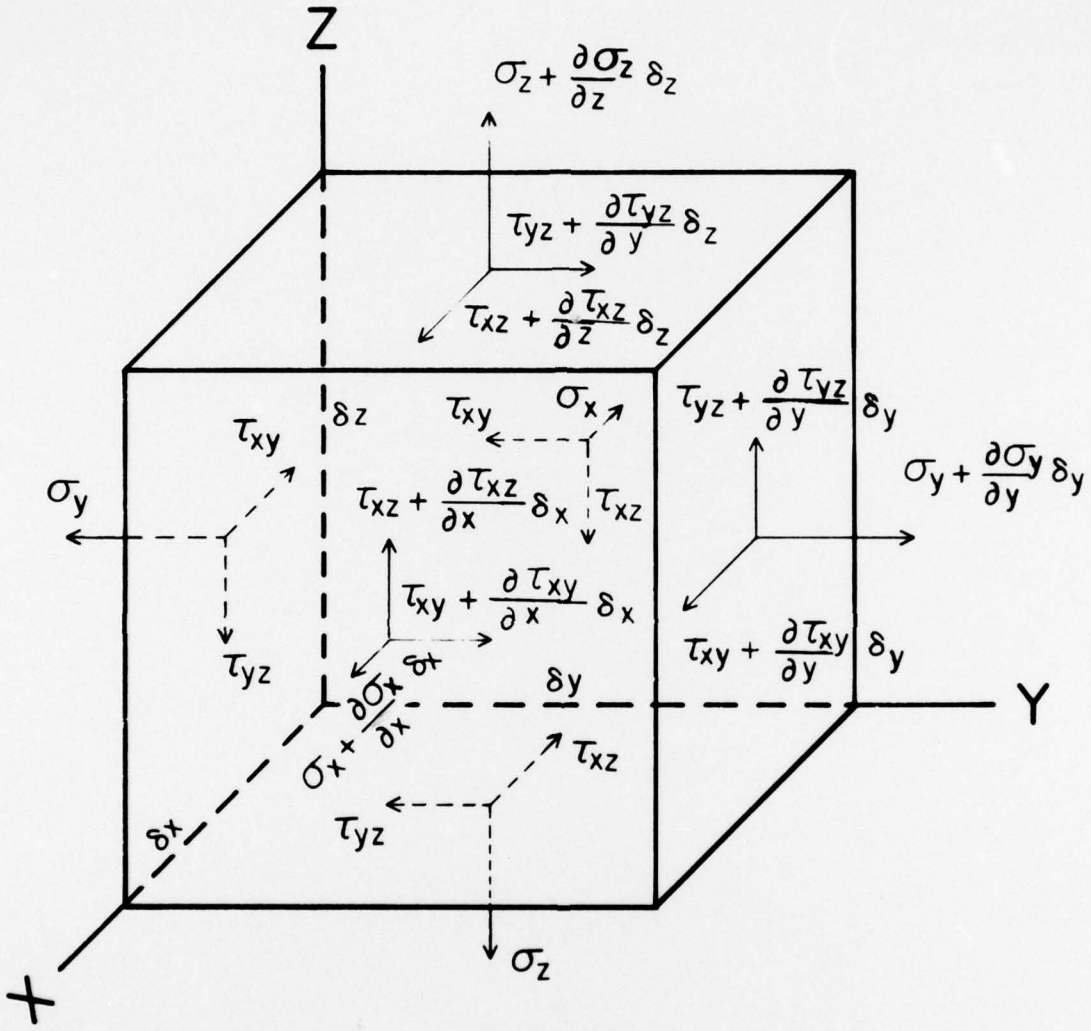

σ_z = STRESS ON Z FACE PARALLEL TO Z AXIS

τ_{ij} = STRESS ON j FACE PARALLEL TO i AXIS

FIGURE 1
STRESSES ON A CUBE

Dividing by $\delta_x \delta_y \delta_z$ yields

$$\frac{\partial \sigma_x}{\partial x} + \frac{\partial \tau_{xy}}{\partial y} + \frac{\partial \tau_{xz}}{\partial z} + X = 0 \tag{2}$$

and similarly, summing forces in the Y and Z directions yields

$$\frac{\partial \sigma_x}{\partial y} + \frac{\partial \tau_{xy}}{\partial x} + \frac{\partial \tau_{yz}}{\partial z} + Y = 0 \tag{3}$$

$$\frac{\partial \sigma_z}{\partial z} + \frac{\partial \tau_{xz}}{\partial x} + \frac{\partial \tau_{yz}}{\partial y} + Z = 0 \tag{4}$$

These equations must be satisfied throughout the body including the boundary surfaces. Expressing the stresses in terms of strains yields the following set of equations: (see Appendix A)

$$\sigma_x = \frac{\upsilon E \mathfrak{L}}{(\upsilon+1)(1-2\upsilon)} + \frac{E\epsilon_x}{\upsilon+1} = \lambda \mathfrak{L} + 2G\epsilon_x \tag{5}$$

$$\sigma_y = \frac{\upsilon E \mathfrak{L}}{(\upsilon+1)(1-2\upsilon)} + \frac{E\epsilon_y}{\upsilon+1} = \lambda \mathfrak{L} + 2G\epsilon_y \tag{6}$$

$$\sigma_z = \frac{\upsilon E \mathfrak{L}}{(\upsilon+1)(1-2\upsilon)} + \frac{E\epsilon_z}{\upsilon+1} = \lambda \mathfrak{L} + 2G\epsilon_z \tag{7}$$

where ν = Poisson's ratio = transverse contraction/elongation

$\epsilon_x, \epsilon_y, \epsilon_z$ = Unit elongations in x, y and z directions

Δ = Volume expansion = $\epsilon_x + \epsilon_y + \epsilon_z$

E = Modulus of elasticity in tension

G = Modulus of rigidity = $E/(\nu+1)2$

λ = Lame's constant = $\nu E/(1+\nu)(1-2\nu)$

For the case of uniform hydrostatic pressure $\sigma_x = \sigma_y = \sigma_z = -P$ and $\Delta = \epsilon_x + \epsilon_y + \epsilon_z$ which is equal to

$$\left(\frac{\sigma_x}{E} - \frac{\nu\sigma_x}{E} - \frac{\nu\sigma_x}{E}\right) + \left(-\frac{\nu\sigma_y}{E} + \frac{\sigma_y}{E} - \frac{\nu\sigma_y}{E}\right) + \left(-\frac{\nu\sigma_z}{E} - \frac{\nu\sigma_z}{E} + \frac{\sigma_z}{E}\right)$$

$$= -3\left(\frac{1-2\nu}{E}\right) P \qquad (8)$$

We can now solve equations (2), (3), and (4) for particle motion by using stress in terms of strain and then strain in terms of displacement as given below.

$$\epsilon_x = \frac{\partial u}{\partial x} \qquad \epsilon_y = \frac{\partial v}{\partial y} \qquad \epsilon_z = \frac{\partial w}{\partial z} \qquad (9)$$

$$\tau_{xy} = G\left(\frac{\partial u}{\partial y} + \frac{\partial v}{\partial x}\right) \quad \tau_{xz} = G\left(\frac{\partial w}{\partial x} + \frac{\partial u}{\partial z}\right) \quad \tau_{yz} = G\left(\frac{\partial v}{\partial z} + \frac{\partial w}{\partial y}\right) \qquad (10)$$

Substituting equation (5) into (2) yields

$$\lambda \frac{\partial \Delta}{\partial x} + 2G \frac{\partial^2 u}{\partial x^2} + G\left(\frac{\partial^2 u}{\partial y^2} + \frac{\partial^2 v}{\partial x \partial y}\right) + G\left(\frac{\partial^2 w}{\partial x \partial z} + \frac{\partial^2 u}{\partial z^2}\right) + X = 0 \qquad (11)$$

which can be written as

$$\lambda \frac{\partial \varepsilon}{\partial x} + G\frac{\partial}{\partial x}\left(\frac{\partial u}{\partial x} + \frac{\partial v}{\partial y} + \frac{\partial w}{\partial z}\right) + G\nabla^2 u + X = 0 \qquad (12)$$

where $\nabla^2 = \frac{\partial^2}{\partial x^2} + \frac{\partial^2}{\partial y^2} + \frac{\partial^2}{\partial z^2}$

Finally, by combining terms and equating this to particle motion, the equation becomes

$$(\lambda+G)\frac{\partial \varepsilon}{\partial x} + G\nabla^2 u + X = \rho \frac{\partial^2 u}{\partial t^2} \qquad (13)$$

Similarly

$$(\lambda+G)\frac{\partial \varepsilon}{\partial y} + G\nabla^2 v + Y = \rho \frac{\partial^2 v}{\partial t^2} \qquad (14)$$

$$(\lambda+G)\frac{\partial \varepsilon}{\partial z} + G\nabla^2 w + Z = \rho \frac{\partial^2 w}{\partial t^2} \qquad (15)$$

where ρ = density.

Now assuming no body forces (<u>i.e.</u>, X=Y=Z=0) and $\mathbf{v}\cdot\nabla\mathbf{v} \ll \dot{\mathbf{v}}$, by differentiating equation (13) with respect to x, equation (14) with respect to y, and equation (15) with respect to z, and adding the resulting equations we can write in vector form[2]

$$\rho \ddot{\vec{\Delta}} = (\lambda+G)\nabla\varepsilon + G\nabla\cdot\nabla\Delta \qquad (16)$$

where $\vec{\Delta} = iu + jv + kw$

This can be written in a more favorable form by using the vector identity

$$\nabla \cdot \nabla \vec{A} = - \nabla \times \nabla \times \vec{A} + \nabla\nabla \cdot A$$

which yields

$$\rho \ddot{\vec{A}} = (\lambda + 2G) \nabla\nabla \cdot \vec{A} - G \nabla \times \nabla \times \vec{A} \qquad (17)$$

This is in a favorable form for the examination of two special cases: (1) $\vec{A}$ is an irrotational vector, ($\nabla \times \vec{A} = 0$) and (2) $\vec{A}$ is a solenoidal vector, ($\nabla \cdot \vec{A} = 0$). In the first case, where $\vec{A}$ is irrotational, equation (17) reduces to

$$\rho \ddot{\vec{\Delta}} = (\lambda + 2G) \nabla^2 \vec{\Delta} \qquad (18)$$

This says that $\vec{\Delta}$ is propagated as a wave with velocity $V_L = \sqrt{\frac{\lambda+2G}{\rho}}$. This wave is termed a longitudinal (or irritational) wave since the only propagated disturbance is directed along the direction of propagation as shown in Appendix B.

In the second case, where $\vec{\Delta}$ is solenoidal, equation (17) reduces to

$$\rho \ddot{\vec{\Delta}} = G \nabla^2 \vec{\Delta} \qquad (19)$$

which says that this displacement component is propagated as a wave with velocity $V_T = \sqrt{G/\rho}$. This displacement is directed at right angles to the direction of propagation as is shown in Appendix B and is known as a transverse or shear wave.

It is important to note that for an ideal fluid the shear modulus, G, is zero and therefore a pure shear wave cannot exist and a longitudinal wave would have a velocity of $V_L = \sqrt{\lambda/\rho}$.

Surface Waves in Elastic Material

We have seen that an elastic solid can support two types of waves: a longitudinal and a transverse or shear wave. What we are primarily interested in, however, is a wave propagating in an elastic material but attached to the boundary of that medium.

In his fundamental paper on surface waves, Lord Rayleigh[3] concerned himself with the question of whether, in an elastic, isotropic semi-infinite solid body, a wave system could exist which decreased exponentially with distance to the boundary plane. The conclusion he arrived at was that such a system is possible in any isotropic medium and that it travels in a direction parallel to the boundary with a velocity which is smaller than the velocity of transverse waves.

This classic paper considered a boundary between an elastic solid and vacuum, the vacuum being incapable of supporting any acoustic wave. Assume a longitudinal wave

with a velocity potential ϕ and a transverse wave with a velocity potential Ψ, in the elastic solid traveling in the x direction. Using the plane z=0 as the boundary plane with z taken positive toward the elastic solid, the following boundary conditions must be satisfied at z=0:

1) Shear stress must vanish, thus

$$\tau_{zx} = G\left(\frac{\partial w}{\partial x} + \frac{\partial u}{\partial z} \right) = 0 \tag{20}$$

$$\tau_{zy} = G\left(\frac{\partial w}{\partial y} + \frac{\partial v}{\partial z} \right) = 0 \tag{21}$$

2) Normal stress must vanish, thus

$$\sigma_z = \lambda \Delta + 2G \frac{\partial w}{\partial z} = 0 \tag{22}$$

Writing the displacements in terms of ϕ and Ψ we obtain

$$u = \frac{\partial \phi}{\partial x} + \frac{\partial \Psi}{\partial z} , \quad w = \frac{\partial \phi}{\partial z} - \frac{\partial \Psi}{\partial x} , \quad v = 0 \tag{23}$$

Assuming that ϕ and Ψ are in the form of

$$\phi = A(z) \exp [ik(x-ct)] \tag{24}$$

$$\Psi = B(z) \exp [ik(x-ct)] \tag{25}$$

where k is the wave number $2\pi/\lambda$ and substituting equation (23) into equations (13), (14), and (15) (the equation of motion) the following conditions result:

$$A(z) = C \exp[-rz] \quad \text{and} \quad B(z) = D \exp[-sz] \tag{26}$$

where C and D are constants and r and s are the positive

values satisfying

$$\frac{r^2}{k^2} = 1 - \frac{c^2}{\alpha^2}, \qquad \frac{s^2}{k^2} = 1 - \frac{c^2}{\beta^2} \tag{27}$$

where $\alpha = V_L$, $\beta = V_T$ and c is the velocity of the surface wave. This derivation is shown in Appendix C.

Now r and s must be positive real numbers in order to fulfill our definition of a surface wave. If either is negative or imaginary the wave amplitude would tend to infinity with depth. A condition, therefore, for the existence of a surface wave as seen from equation (27) is that c^2 shall be less than β^2 and less than α^2. If these conditions are not satisfied ϕ or Ψ or both will not represent a surface wave but a wave traveling upwards or downwards.[4]

Using equations (23), (24), and (25) the boundary condition given by equation (20) now becomes

$$G\left(\frac{\partial u}{\partial z} + \frac{\partial w}{\partial x}\right) = G\left(2\frac{\partial^2 \phi}{\partial x \partial z} + \frac{\partial^2 \psi}{\partial z^2} - \frac{\partial^2 \psi}{\partial x^2}\right) = 0 \tag{28}$$

Since in an elastic solid the shear modulus G is not equal to zero, we can write this boundary condition with the use of equations (24), (25), and (26) as

$$-2ikrC\frac{\exp[-rz]}{\exp[-sz]} + D(s^2 + k^2) = 0 \tag{29}$$

and at the plane z=0

$$-2ikrC + D(s^2 + k^2) = 0. \tag{30}$$

Operating on the boundary condition given in equation (22) in the same manner we obtain

$$\lambda\varepsilon + 2G\frac{\partial w}{\partial z} = \lambda\nabla^2\phi + 2G\left(\frac{\partial^2\phi}{\partial z^2} - \frac{\partial^2\psi}{\partial x\partial z}\right) \tag{31}$$

which at the plane z=0 reduces to

$$\left[-\lambda k^2 + (\lambda + 2G)r^2\right] C + 2Giks D = 0 \tag{32}$$

Equations (30) and (32) can then be combined, as is done in Appendix D, to yield the Rayleigh wave equation

$$\frac{c^2}{\beta^2}\left[\frac{c^6}{\beta^6} - 8\frac{c^4}{\beta^4} + \frac{c^2}{\beta^2}\left(24 - 16\frac{\beta^2}{\alpha^2}\right) - 16\left(1 - \frac{\beta^2}{\alpha^2}\right)\right] = 0 \tag{33}$$

This is a quadratic in terms of c^2/β^2. One of the roots is obviously equal to zero. Hence, from equations (27) and (30) we have r=k=s, C=-iD and then substituting this into equations (24), (25), and (26) and using the results in equation (23) we find that u=v=w=0. Thus there is no wave at all and this is not acceptable.

Discarding this factor and writing $\frac{\beta^2}{\alpha^2}$ as $\frac{(1-2\nu)}{2(1-\nu)}$ the Rayleigh equation now becomes

$$\left(\frac{c^2}{\beta^2}\right)^3 - 8\left(\frac{c^2}{\beta^2}\right)^2 + 8\left[3 - \left(\frac{(1-2\nu)}{(1-\nu)}\right)\right]\frac{c^2}{\beta^2} - 16\left(1 - \frac{1-2\nu}{2(1-\nu)}\right) = 0 \qquad (34)$$

In general this equation has one real root and two complex roots which must be discarded for reasons previously discussed. Each medium has its own Poisson ratio which, when inserted into equation (34), will determine the acceptable value for c^2/β^2. Once this ratio is determined the process to determine particle motion is straight forward and is as follows:

1) Determine β^2 from $\beta^2 = G/\rho$
2) Find c from the solution for c^2/β^2
3) Using equation (27) find r and s in terms of k
4) Using equation (23) find u and w in terms of C, D, k and z

Proceeding in this manner and taking the real part of the resulting expression, the displacements u and w may be written as

$$u = K(\exp[-rz] - M \exp[-sz]) \sin k\,(x - ct) \qquad (35)$$

$$w = K(N \exp[-rz] - O \exp[-sz]) \cos k\,(x - ct) \qquad (36)$$

where K is a constant and M, N, and O depend upon β, C, D,

r and s. These may also be written as[5]

$$u = K\left\{ \frac{2(1 - c^2/\alpha^2)^{1/2}\,(1 - c^2/\beta^2)^{1/2}}{(2 - c^2/\beta^2)} \exp[-k(1 - c^2/\beta^2)]^{1/2} z \right.$$

$$\left. - \exp[-k(1 - c^2/\beta^2)]^{1/2} z \right\} \sin(wt-kx) \quad (37)$$

$$w = -K\left\{ \frac{2(1 - c^2/\beta^2)^{1/2}}{2 - c^2/\beta^2} \exp[-k(1 - c^2/\beta^2)^{1/2}]z \right.$$

$$\left. - (1 - c^2/\beta^2) \exp[-k(1-c^2/\beta^2)^{1/2} z \right\} \cos(wt - kx) \quad (38)$$

In Figure 2 on the following page are plotted the particle orbits in a surface wave as well as the Poisson's ratio, α/β, and c/β with which they are associated. Also with reference to equation (36), the depth at which u=0 is also noted. All of the magnitudes of displacement are referred to the value of the transverse component w at the surface of the solid. As is shown in Figure 2, the particles near the surface travel in elliptical orbits in a clockwise direction as viewed in a wave moving left to right; at a certain depth below the surface the particles oscillate in a vertical line; and at still greater depths the particles travel in elliptical orbits of diminishing dimensions in which the direction of rotation is counterclockwise.

From an energy standpoint, about 95% of the energy is contained within 1 wavelength of the surface.[5] The experimental results of Cook and VanValkenberg[5] are shown in Figure 3.

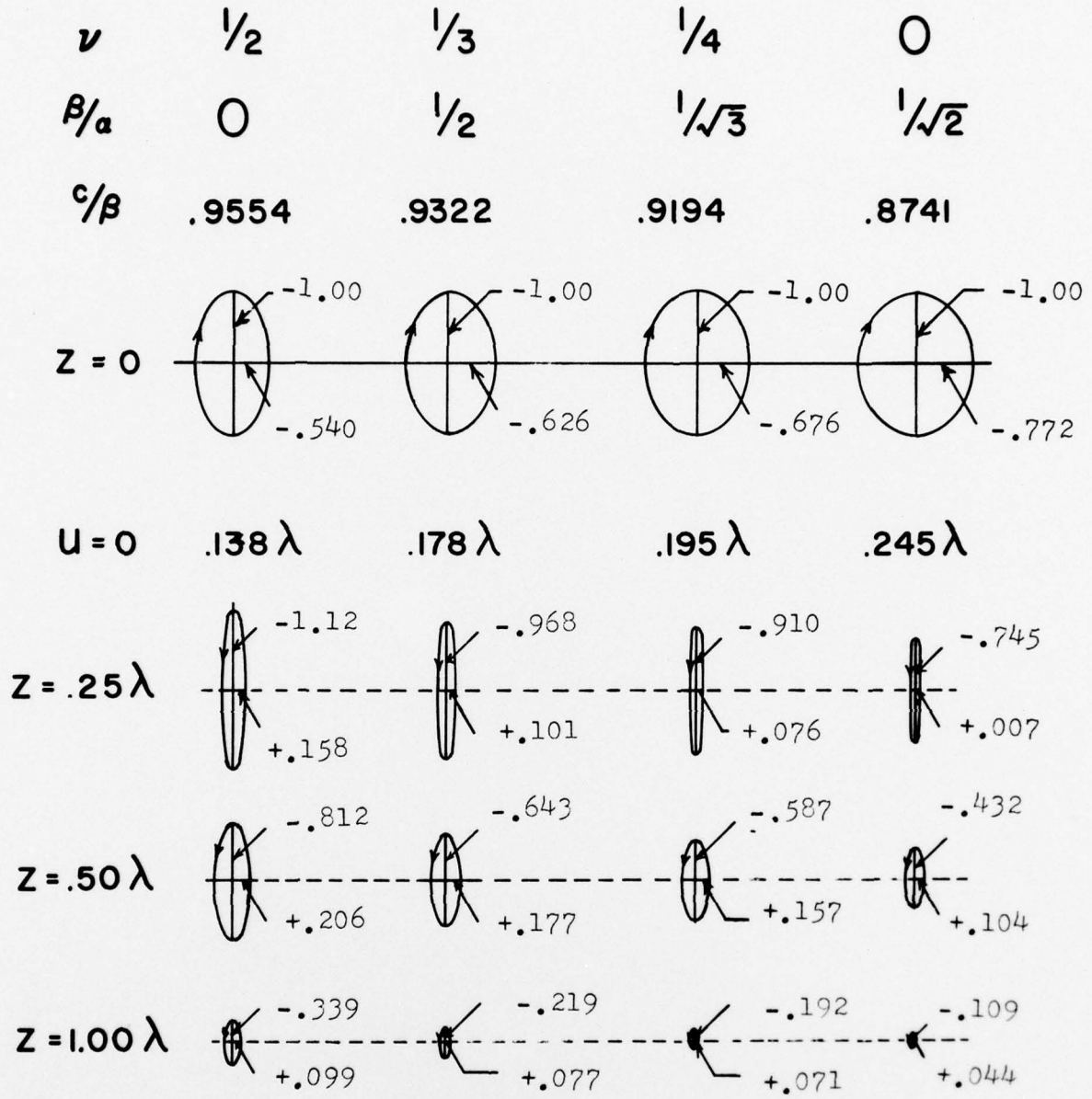

FIGURE 2 PARTICLE ORBITS IN A SURFACE WAVE

Reprinted from Figure 3 of "Surface Waves at Ultrasonic Frequencies" by E. Cook and H. Van Van Valkenberg with some additions.

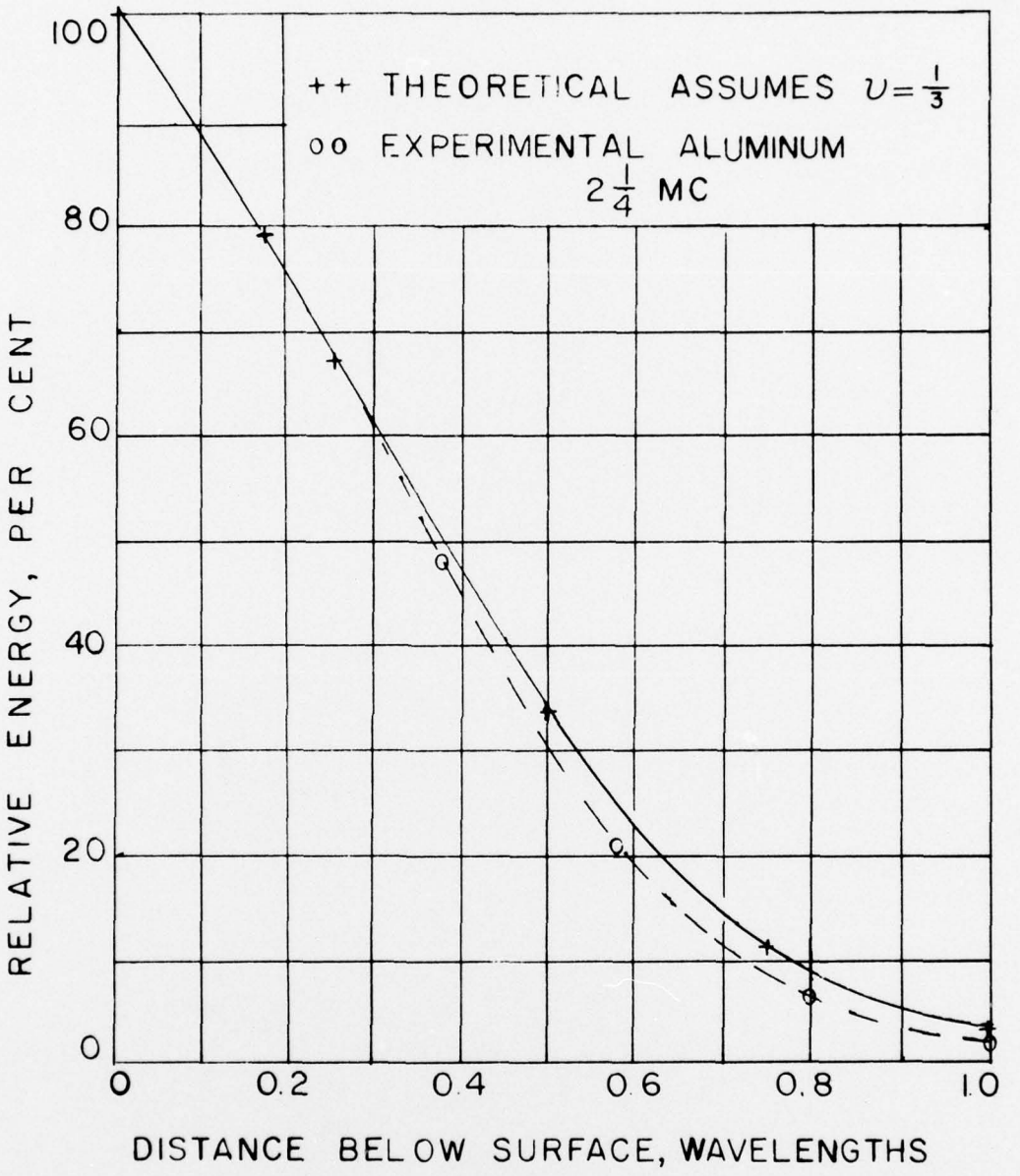

FIGURE 3

ENERGY OF SURFACE WAVES (PER CENT) versus DISTANCE BELOW SURFACE (WAVE LENGTHS)

Reprinted from Figure 6 of "Surface Waves at Ultrasonic Frequencies" by E. Cook and H. Van Valkenberg

III. SURFACE WAVES ON A FLUID LOADED BOUNDARY

In the preceeding section we have determined the surface wave motion for a wave attached to a boundary between a solid and vacuum. What we desire, however, is the particle motion for a surface wave attached to the boundary between a solid and a liquid.

The procedure here is somewhat different than that of the preceeding section. This is brought about as an easy way to handle the stress at the boundary which are now altered by the appearance of a wave in the liquid medium.[6] One can separate the wave in the solid into its longitudinal and transverse components and after determining the stress on the boundary caused by each, equate them to produce the proper boundary conditions. This will then yield an equation for the wave traveling along the surface of the medium.

In an ideal fluid the modulus of rigidity, G, is equal to zero. Therefore, the fluid can support a longitudinal wave but not a shear wave. This means that the stress normal to the boundary will be continuous while the stress parallel to the boundary must vanish. Using the coordinate system as shown in Figure 4 a longitudinal wave of the form $\phi = A_1 \exp[iv(t - \frac{x \sin\theta_1 + z \cos\theta_1}{\alpha})]$ exerts a stress on the plane z=0 equal to

$$\tau_{zx} = -iv\rho\alpha A_1 \, 2 \sin^2\theta_1' \cot\theta_1 \tag{39}$$

$$\sigma_z = -iv\rho\alpha A_1 \cos 2\theta_1' \tag{40}$$

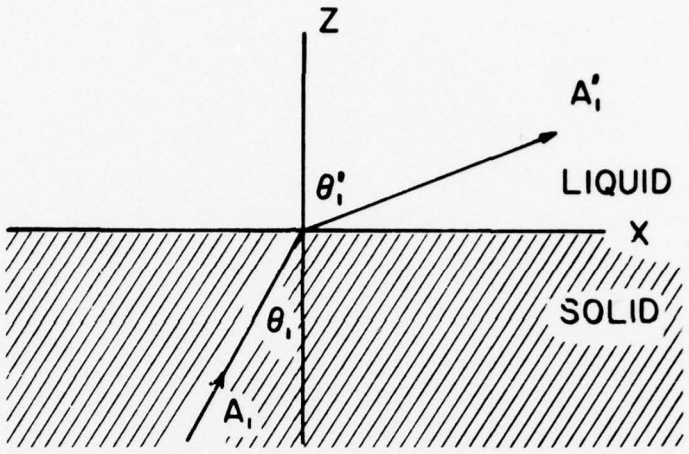

FIGURE 4

COORDINATE SYSTEM FOR LONGITUDINAL WAVE

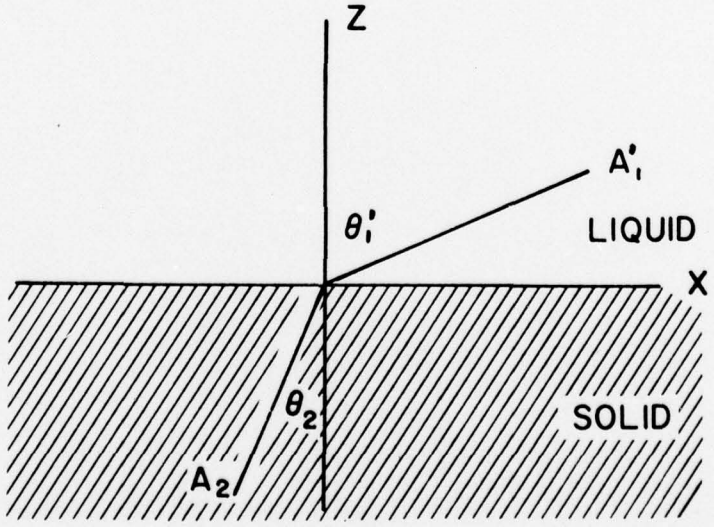

FIGURE 5

COORDINATE SYSTEM FOR SHEAR WAVE

where the phase velocities have been omitted. These are obtained from equations (20) and (22) and the use of Snell's Law $\sin \theta_1' = \beta/\alpha \ (\sin \theta_1)$. (41)

In the liquid medium a wave

$$\phi' = A_1' \exp[iv \ (t - \frac{x \sin \theta_1' + z \cos \theta_1'}{\alpha'})] \tag{42}$$

appears, which is connected with the movement of the solid body by the condition that the vertical motion only must be continuous. From this condition it follows that

$$\frac{\sin\theta_1'}{\alpha'} = \frac{\sin\theta_1}{\alpha} \quad \text{and} \quad A_1' \cos \theta_1' = A_1 \cos \theta_1. \tag{43}$$

This wave in the fluid exerts on the interface a vertically directed stress

$$\sigma_z = -iv\rho'\alpha'A_1' = -iv\rho'\alpha A \frac{\cot\theta_1}{\cot\theta_1'} \tag{44}$$

This results in stress differences at the boundary equal to

$$\Delta\tau_{zx} = -iv\rho\alpha A_1 \ 2 \sin^2\theta_1' \cos \theta_1 \tag{45}$$

$$\Delta\sigma_z = -iv\rho\alpha A_1 (\cos 2\theta_1' - \frac{\rho' \cot \theta_1}{\rho \cot \theta_1'}) \tag{46}$$

where Δ now denotes infinitesimal change. These stress differences can be represented by a vector in the direction given by

$$\frac{\Delta\tau_{zx}}{\Delta\sigma_z} = \frac{2 \sin^2\theta_1' \cot\theta_1}{\cos 2\theta_1' \quad \frac{\rho' \cot\theta_1}{\rho \cot\theta_1'}} \tag{47}$$

The transverse wave in the solid may be handled in the same way. Let Ψ be of the form

$A_2 \exp[iv(t - \frac{x \sin\theta_2 + z\cos\theta_2}{\beta})]$ traveling in the solid medium and incident upon the boundary as shown in Figure 5. The stresses on the boundary plane z=0 caused by this wave in the solid are by use of equations (20) and (22)

$$\tau_{zx} = -iv\rho\beta A_2 \cos 2\theta_2 \tag{48}$$

$$\sigma_z = +iv\rho\beta A_2 \, 2\sin^2\theta_2 \cot\theta_2 \tag{49}$$

The accompanying wave in the fluid is propagated in the direction θ_1' as given by

$$\frac{\sin\theta_1'}{\sin\theta_2} = \frac{\alpha'}{\beta} \tag{50}$$

with A_1' satisfying $A_1'\cos\theta_1' = -A_2 \sin\theta_2$. (51)

This wave exerts a stress normal to the boundary equal to

$$\sigma_z = \frac{iv\rho'\beta A_2}{\cot\theta_1'} \tag{52}$$

The stress differences then caused by this transverse wave are

$$\Delta\tau_{zx} = -iv\rho\beta A_2 \cos 2\theta_2 \tag{53}$$

$$\Delta\sigma_z = +iv\rho\beta A_2 (2\sin^2\theta_2 \cot\theta_2 - \frac{\rho'}{\rho\cot\theta_1'}) \tag{54}$$

The stresses due to the transverse wave can similarly be represented by a vector in the direction given by

$$\frac{\Delta\tau_{zx}}{\Delta\sigma_z} = \frac{\cos 2\theta_2}{2\sin^2\theta_2 \cot\theta_2 - \frac{\rho'}{\rho\cot\theta_1'}} \tag{55}$$

As the normal stress on the interface must be continuous the stress differences have to disappear which is only possible if the two stress differences as given by equations (47) and (55) are in the same direction. This leads to

$$\frac{2\sin^2\theta_2\cot\theta_1}{\cos 2\theta_2 - \frac{\rho'\cot\theta_1}{\rho'\cot\theta_1'}} = -\frac{\cos 2\theta_2}{2\sin^2\theta_2\cot\theta_2 - \frac{\rho'}{\rho\cot\theta_1'}} \tag{56}$$

which if expanded yields

$$\cos^2 2\theta_2 + 4\sin^4\theta_2 \cot\theta_1 \cot\theta_2 - \frac{\rho'\cot\theta_1}{\rho\cot\theta_1'} = 0 \tag{57}$$

Although this condition is necessary it is not sufficient. The stress on the interface disappears if A_1 and A_2 satisfy the equation $\Delta\tau_{zx_{long}} = \Delta_{zx_{trans}}$ or

$$\alpha A_1 2\sin^2\theta_2\cot\theta_1 = \beta A_2\cos 2\theta_2 \tag{58}$$

Equation (57) determines the directions of the three-wave system possible in two media, one of which is a liquid. Such a system will be a kind of Rayleigh wave if the waves

decrease exponentially with increasing distance from the interface. In this case $\cot\theta_1$ and $\cot\theta_2$ are positive imaginary and $\cot\theta_1'$ is negative imaginary. Now by use of Snell's law and knowing that c is less than β, equation (57) becomes

$$(2\beta^2 - c^2)^2 - \frac{4\beta^3}{\alpha}\left[(\beta^2 - c^2)(\alpha^2 - c^2)\right]^{1/2} + \frac{\rho'\alpha'}{\rho\alpha} c^4\left[\frac{(\alpha^2 - c^2)}{(\alpha'^2 - c^2)}\right]^{1/2} = 0 \qquad (59)$$

This is the Rayleigh wave equation as expressed in equation (33) but in a different form and also includes the case where the second medium has a non-zero density.

One root is again $c^2 = 0$ which as before is not acceptable. For small values of c^2 the left hand side of equation (59) is negative and if c^2 is taken equal to the smallest of the three velocities (which is either β or α') the left hand side will now be positive. There will therefore always be a root such that c^2 will be less than α^2.

For small values of $\rho'\alpha'/\rho\alpha$ the transfer of energy is also small and propagation will not be much different from that in the preceeding discussion where a vacuum replaced the liquid. However, in the case where α' is much smaller than β and also smaller than c the third term in equation (59) is imaginary. This produces a pair of complex roots with real parts equal to c.

The corresponding wave system is now as before, but the imaginary part of the roots gives rise to a slight

exponential decrease with distance of propagation and a small sinusoidal variation in the vertical direction.(6)

Another factor of great importance is that a surface wave can only be propagated in a substance whose thickness is larger than two surface wavelengths.(7) Throughout the preceeding sections it was assumed that the elastic medium was an infinite halfspace, but in any experiment or practical case this cannot occur. As the thickness of the bar increases the distance of possible surface wave propagation also increases. For a thickness $h = 3\lambda_r$ the distance of propagation is about $20\lambda_r$, for $h = 5\lambda_r$ it is already $2000\lambda_r$.(3)

IV. EXPERIMENTAL ARRANGEMENT

The experiment was conducted by launching surface waves on an aluminum bar underwater and then measuring the pressure pattern in the liquid at the end of the bar. The experimental arrangement shown in block diagram form in Figure 6 consisted of two main parts: the acoustic equipment and the electronics.

The steel tank in which the experiment was carried out is 6 1/4 feet long and 2 1/4 feet in width and depth. The tank is lined on the bottom, ends and sides with two inch thick rubberized hair. Measurements indicated a normal reflection loss of 26 db for the material at a frequency of 1 mcps[8]. Since a pulse technique was used the absorption was quite sufficient to handle all possible reflections. The tank was filled with fresh tap water.

As was asserted earlier, in order to transmit a significant percentage of the energy into the fluid, the ratio $\rho'\alpha'/\rho\alpha$ should be as large as possible. With reference to Table 1, giving some important acoustical properties of metals and alloys, it is seen that except for bismuth and magnesium, aluminum appears to be the best choice for a favorable amount of energy transmission into the water. Another factor dictating this choice was that bars of bismuth or magnesium would be quite expensive. A photograph of the bars used as well as pictures of the tank and electronic equipment are shown in Figures 7,8 and 9.

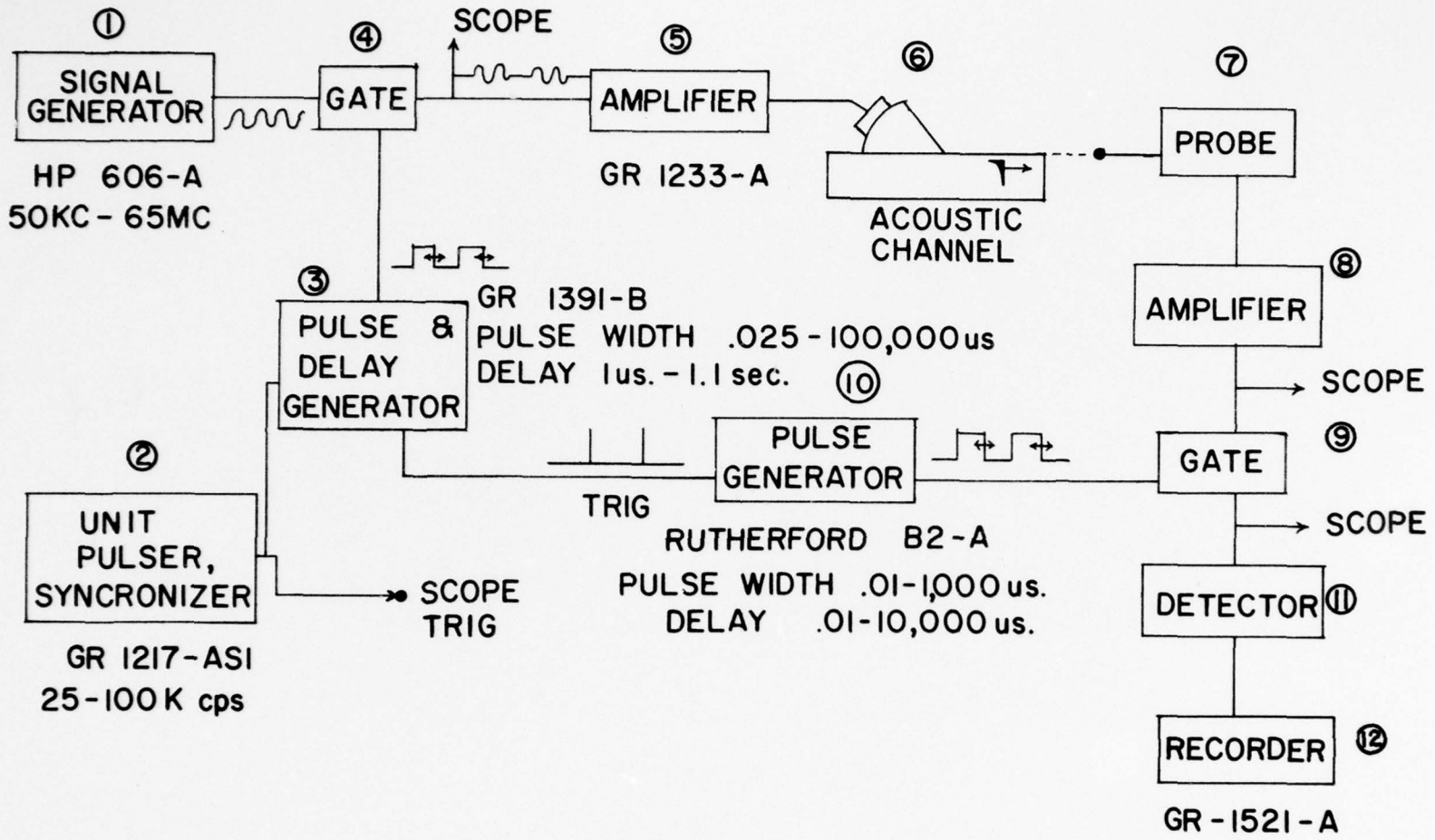

FIGURE 6 DIAGRAM OF THE EXPERIMENT

TABLE I

PROPERTIES OF METALS AND ALLOYS

Material	"	Specific Gravity	$V_{long.}$ ft./sec.	$\frac{\rho_{H_2O} V_{H_2O}}{\rho_{Met.} V_{Met.}}$
Aluminum	.34	2.7	16,740	.11
Alnico	.32	7.0	16,072	.04
Antimony	.33	6.6	11,152	.07
Beryllium	.01	1.8	27,552	.10
Bismuth	.35	9.7	2,624	.20
Brass	.33	7.7	11,152	.06
Bronze Phosphor	.35	8.8	12,136	.05
Cadmium	.30	8.6	8,200	.07
Cobalt	.30	8.7	15,416	.04
Copper	.35	8.9	11,670	.05
Duraluminum	.33	2.8	16,400	.11
German Silver	.37	8.1	12,464	.05
Gold	.42	19.3	5,717	.04
Iridium	.33	22.4	4,920	.05
Iron	.28	7.8	16,600	.04
Lead	.45	11.3	15,700	.03
Magnesium	.33	1.7	15,100	.19
Monel	.32	8.8	14,760	.04
Nickel	.31	8.8	16,072	.04
Palladium	.39	12.0	10,496	.04
Platinum	.39	21.4	8,815	.03
Rhodium	.34	12.4	16,072	.03
Silver	.38	10.5	8,553	.06
Steel C .08	.37	7.7	16,400	.04
Tantalum	.31	16.6	11,152	.03
Tin	.36	7.2	8,200	.08
Tungsten	.17	19.0	14,104	.02
Zinc	.43	7.1	12,146	.06

Three of the four bars used were machined on all six faces leaving the remaining bar to compare the effect of surface roughness on surface wave propagation.

The transducer used to launch the surface waves was a barium titanate plate in a plexiglass holder which was mounted on a plexiglass wedge as shown in Figure 10. The basic equation for surface wave creation is, with reference to Figure 10,

$$\sin \theta_i = \sin^{-1} \frac{V_{\text{longitudinal wave in wedge}}}{V_{\text{surface wave in bar}}} \quad (60)$$

and therefore $V_{\text{longitudinal wave in the wedge}}$ must be less than $V_{\text{surface wave in the solid}}$. A sector of a circle rather than a triangular wedge with a fixed angle was used in order to facilitate the use of different metallic substances if this was desired. Acoustical contact between the transducer housing, wedge and bar was maintained by a film of castor oil. The loss in acoustic pressure between the transducer and bar (a distance of 4 inches) at a frequency of 760 kc, which was used in the experiment, is approximately 20 db[10]. For the case of the plexiglass wedge having a longitudinal wave velocity of 9068 ft./sec. and aluminum having a surface wave velocity of 9769 ft./sec. the optimum incidence angle is 68° which was kept constant throughout the investigation. This angle is the solution to equation (60) and is the critical wedge angle at which maximum conversion of a longitudinal wave

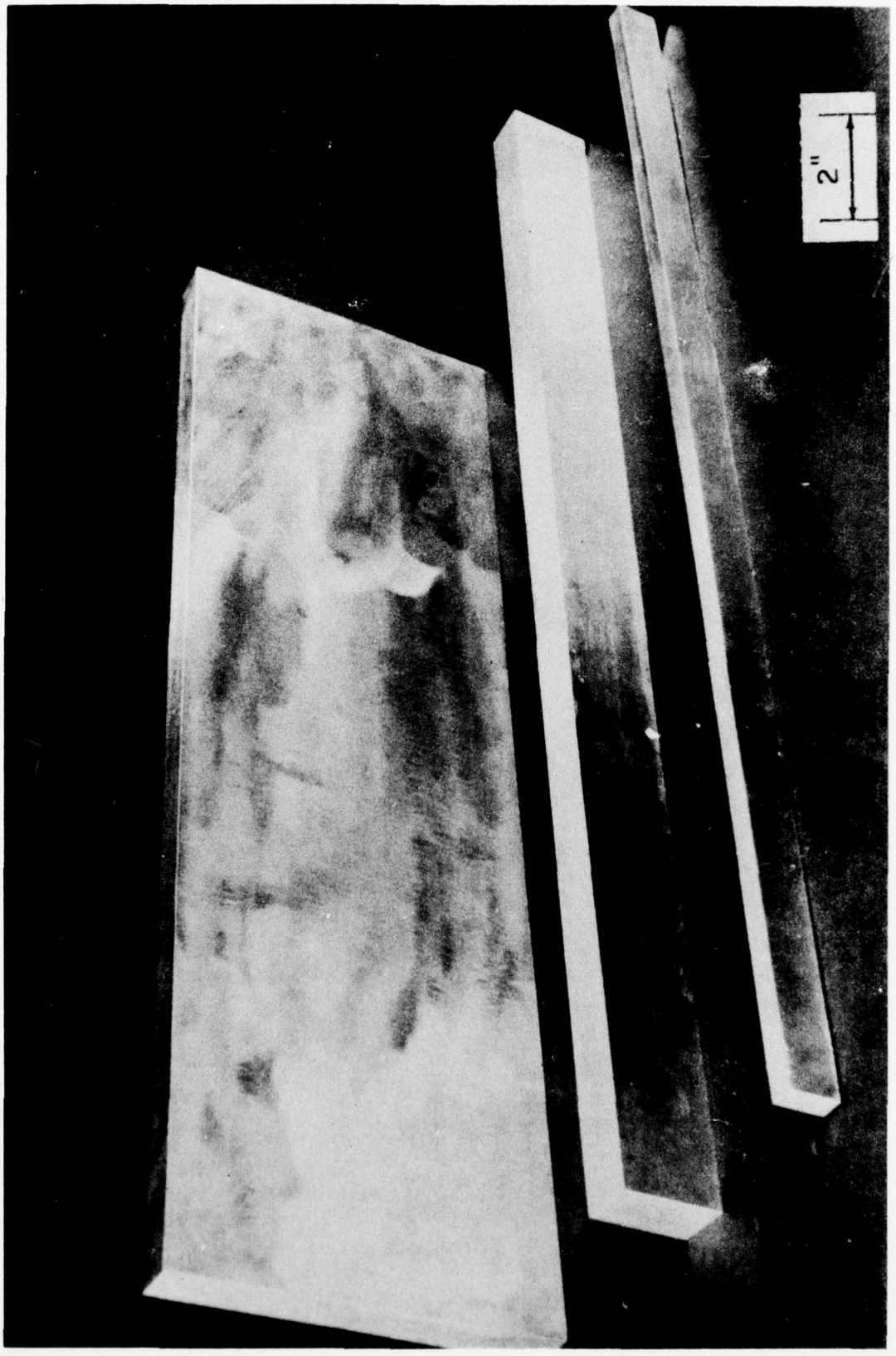

FIGURE 7 BARS USED IN THE EXPERIMENT

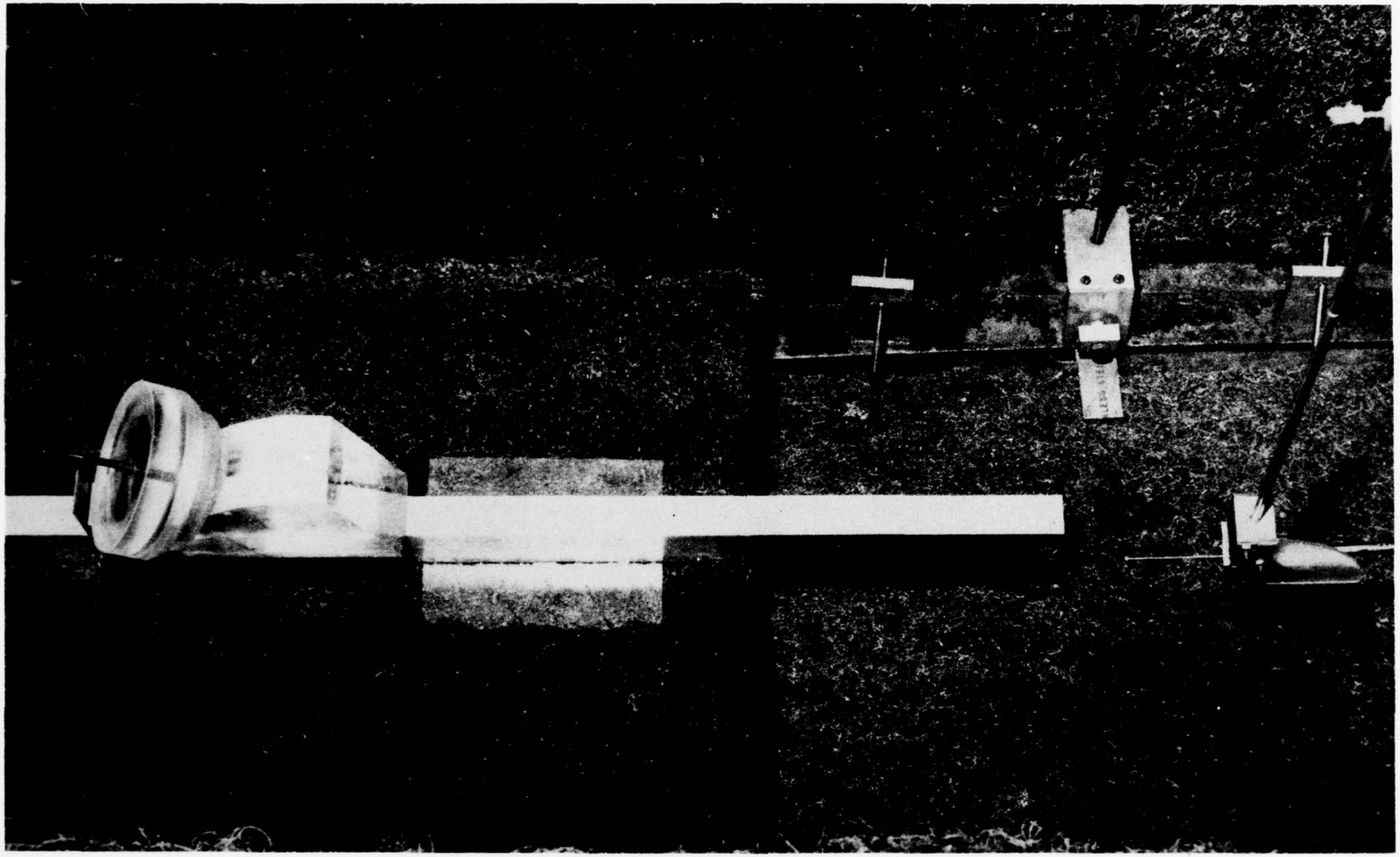

FIGURE 8 EXPERIMENTAL ARRANGEMENT

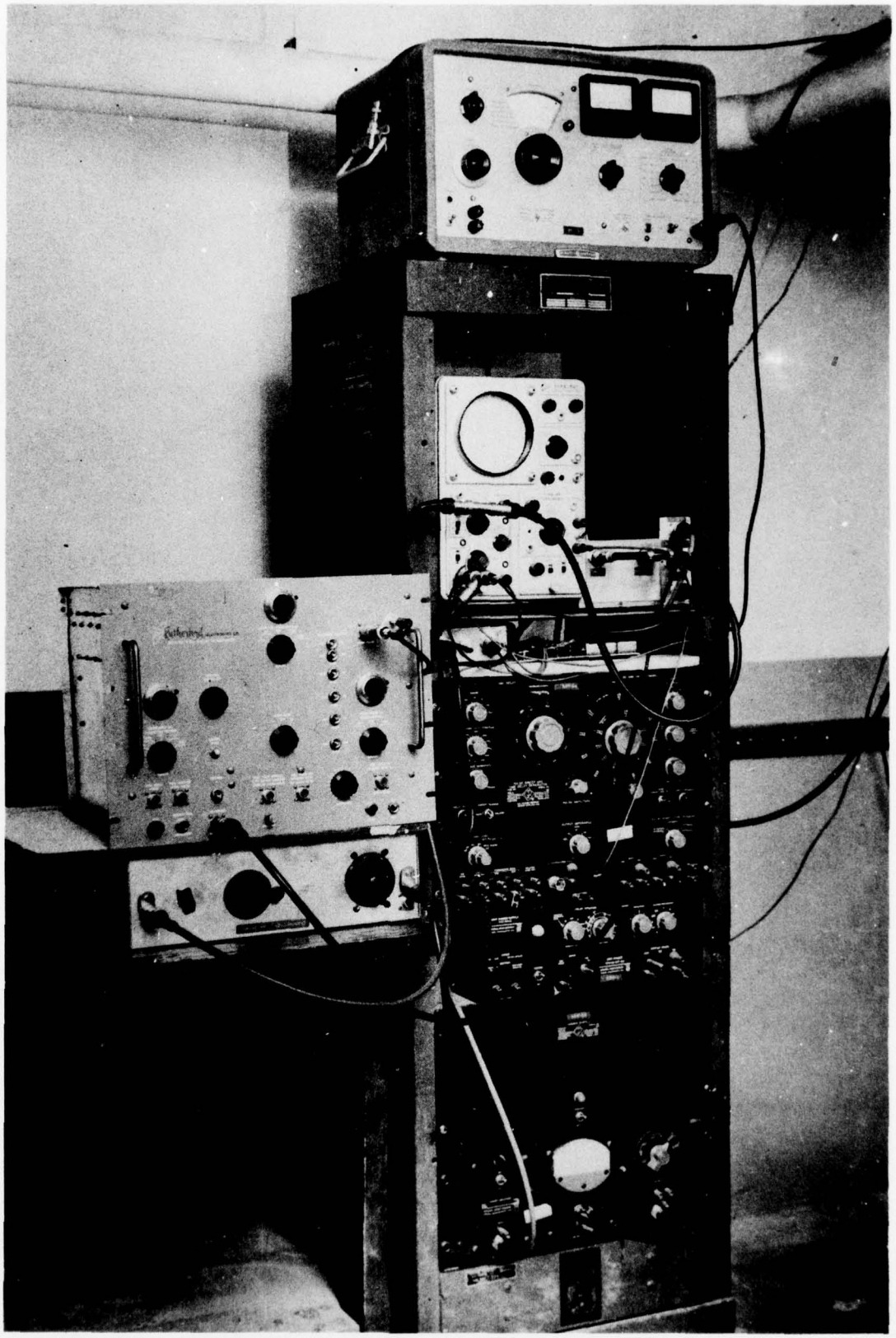

FIGURE 9 ELECTRONIC ARRANGEMENT

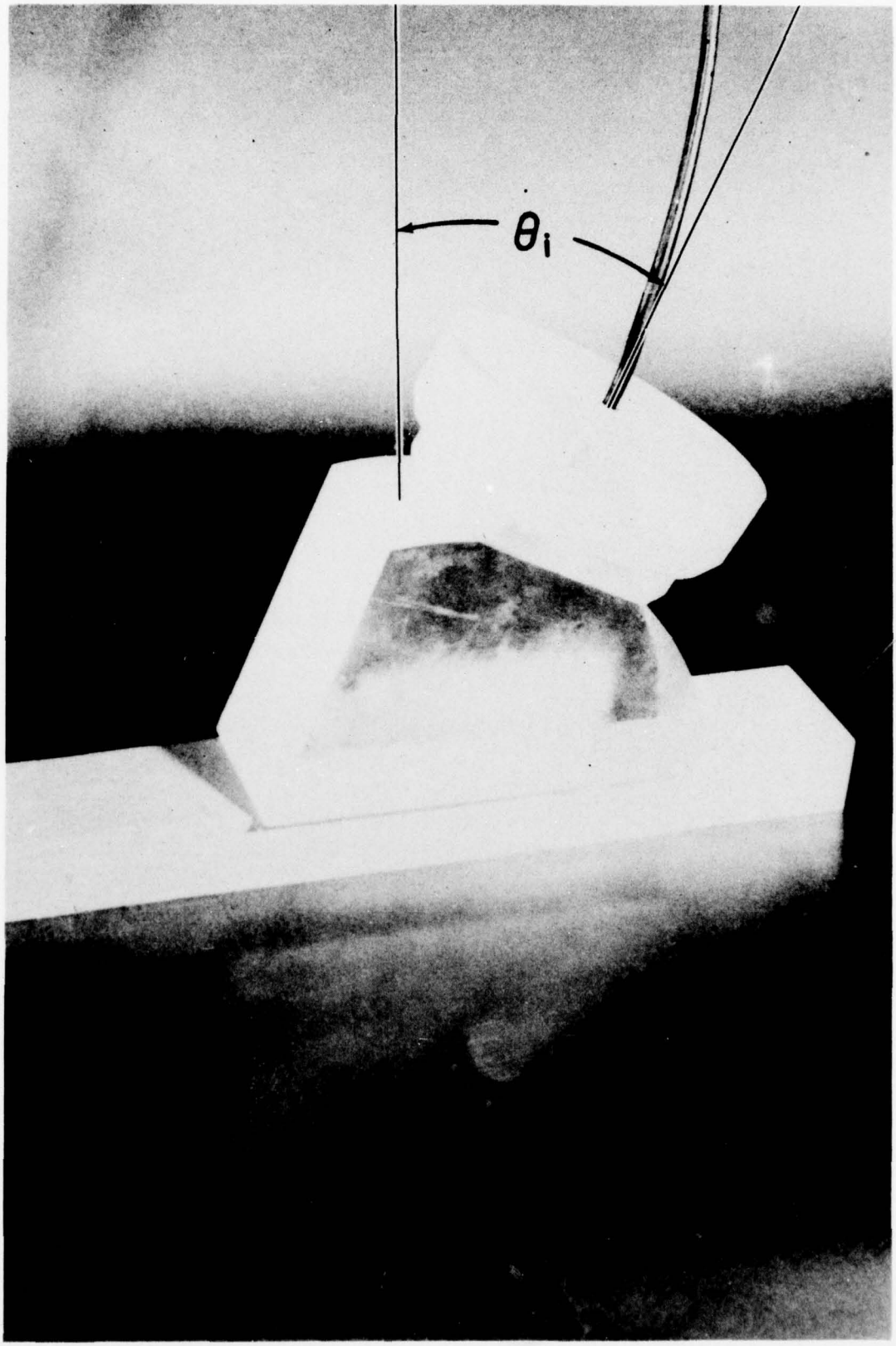

FIGURE 10 TRANSDUCER AND WEDGE

into a surface wave occurs[11]. This transformation occurs because the wedge, acting as a prism, sets up at the boundary a periodic disturbance with a spatial period of λ_r. Since the incident angle is greater than the angle of total internal reflection for both longitudinal and shear waves, there results an inhomogeneous wave known as a surface wave. The wedge method was also used because in all methods of surface wave excitation except the wedge method the resulting wave pulse has a longer duration than the exciting voltage[12].

The receiving probe is a Glennite Ultrasonic Probe type UP-800 manufactured by Gulton Industries, Inc. of Metuchen, N. J.. The sensitive element of this unit is a barium titanate ceramic cylinder having a diameter and length of 1/16 th of an inch. At a frequency of 760 kc the sensitivity of the probe is -135 db referred to 1 volt/dyne/square centimeter.

The electronic arrangement is included in Figure 6 in block diagram form. The output waveform is a pulsed sine wave with a variable carrier frequency. The frequency and amplitude of the excitation are controlled by the Hewlett Packard Signal Generator model 606-A [1]* while the pulse repetition rate is determined by the General Radio Unit Pulser model 1217-AS1 [2], which also acts as the synchronizing device for the experiment. The

---

* Numbers in brackets refer to circled numbers in Figure 6.

frequency rage is 50 kc to 65 mc and the repetition rate is adjustable from 25 cps. to 100k cps.. The pulse duration is determined by the General Radio Pulse, Sweep and Time Delay Generator model 1391-B [3], with a variable pulse width from 0.025 usec. to 100,000 usec.. A gate [4] whose schematic diagram is shown in Figure 11 is used to modulate the sine wave. After gating, the pulsed sine wave is amplified by the General Radio Power Amplifier model 1233-A [5] with a gain of 60$\pm$ 1/2 db from 20 cps. to 2 mcps. and is then transmitted by the barium titanate transducer [6]. The output wave shape has a signal to noise ratio of 500.

The signal produced by the receiving probe [7] is amplified by a specially built small signal, high input impedance, wideband amplifier [8] with a voltage gain of 100 db. The schematic of the amplifier, which has a minimum signal requirement of 2 uvolt, is shown in Figure 12. This signal is then gatted [9] so as to pick out only that part of the received wave produced by the surface wave. This gate is identical with the one used in forming the transmitted signal, but is now modulated by a square wave produced by the Rutherford Electronics Square Wave Generator model B-2A [10]. This generator is triggered by the Pulse, Sweep and Time Delay Generator and can be adjusted to produce a square pulse of variable width and variable time delay after being triggered. The resulting signal is then just the wave produced by the surface wave

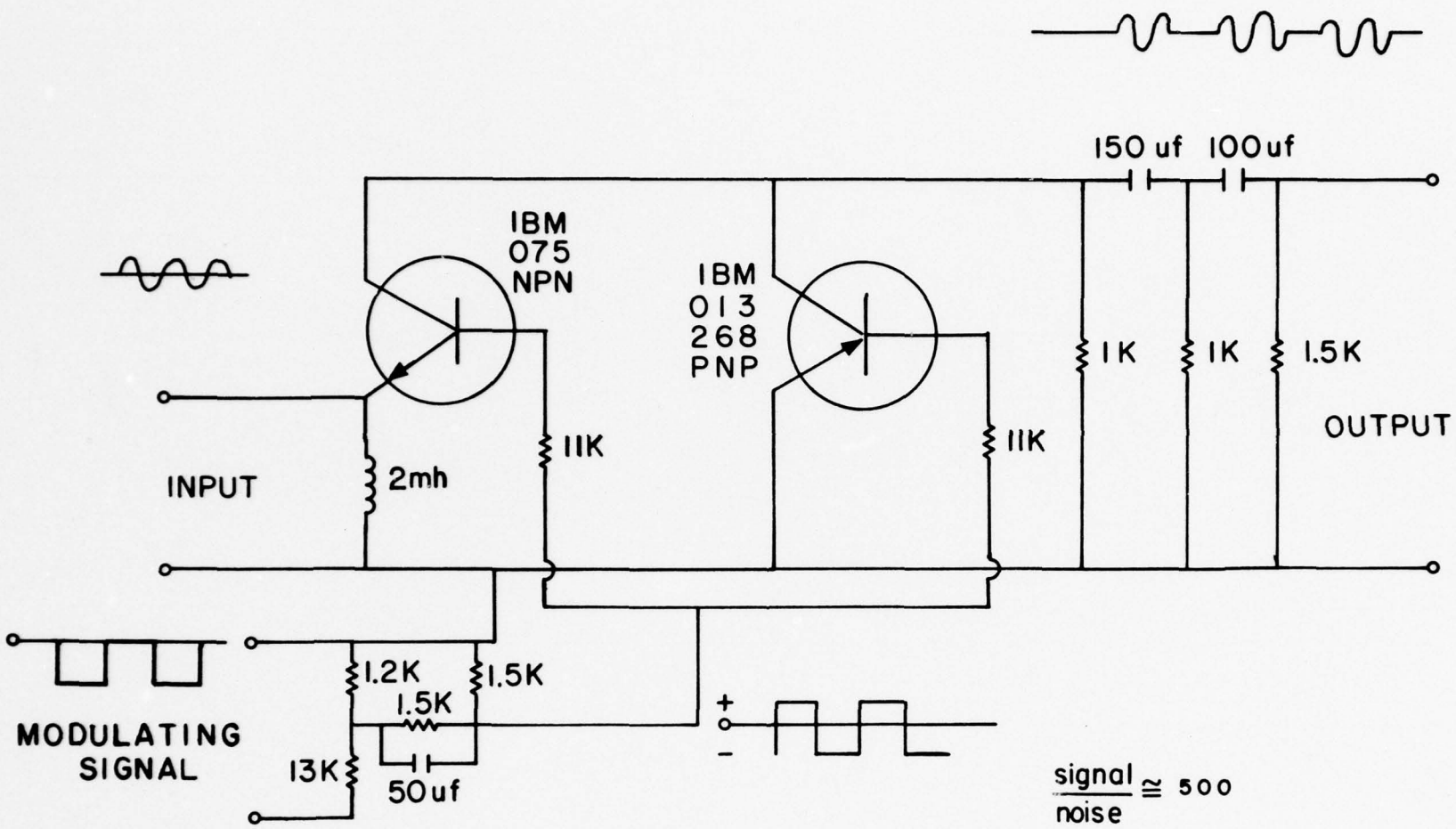

FIGURE 11 SCHEMATIC OF GATING CIRCUIT

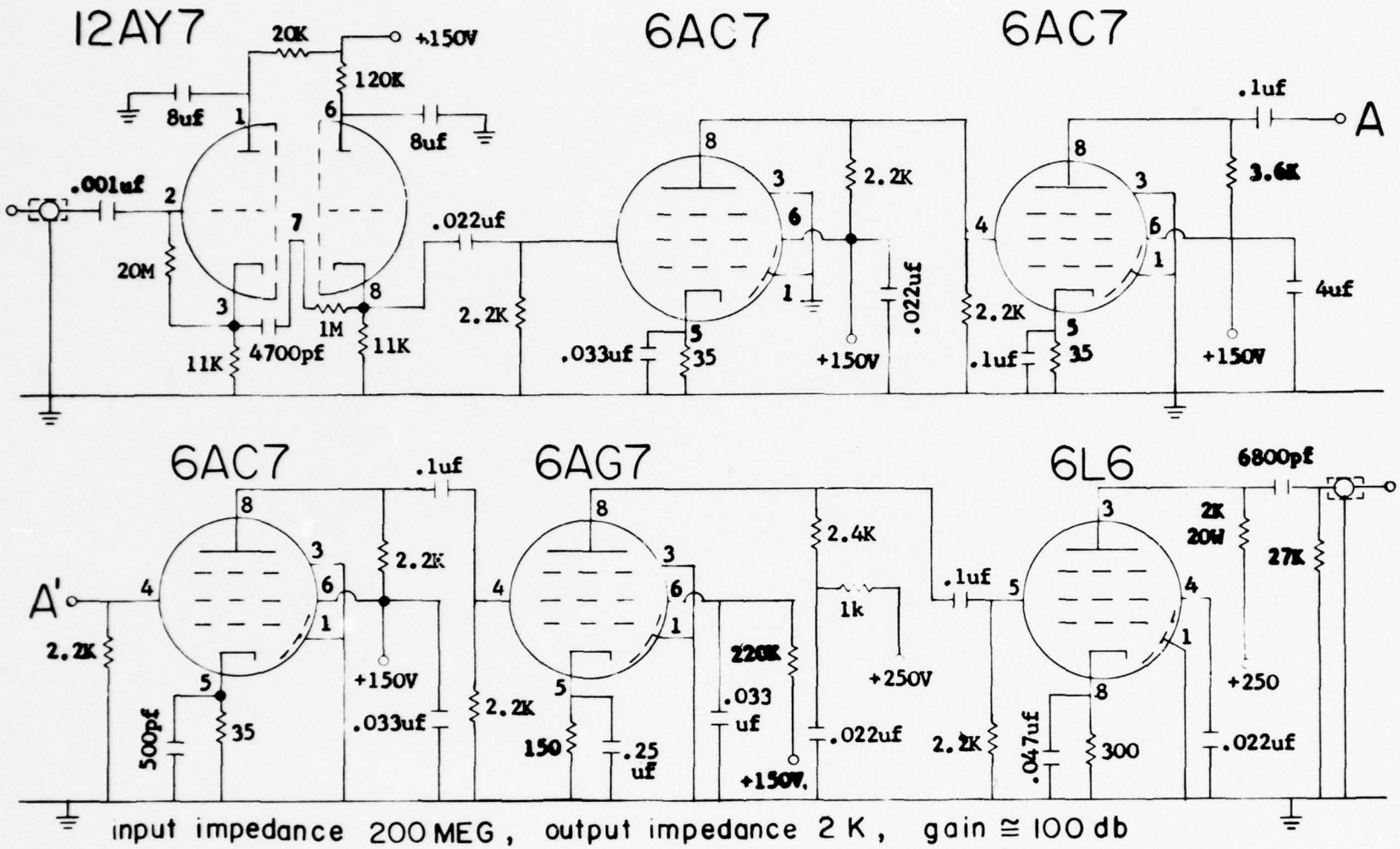

FIGURE 12 SCHEMATIC OF RECEIVING AMPLIFIER

when the variable gate is adjusted correctly. This is then detected by a peak detector [11] and then recorded on the General Radio Graphic Level Recorder model 1521-A [12]. An oscilloscope, which is triggered by the Unit Pulser, is used to view the waveshape at any point in the system. This is used to measure pulse width and amplitude, to help determine wave velocities by noting time differences and to aid in positioning the gate [9]. The overall sensitivity of the receiving system was such as to produce an output of .1 volt dc/ 80 microbar.

V. PROCEDURE

In order to obtain the greatest sensitivity it was necessary to choose an optimum frequency and select the proper incidence angle for the transmitting transducer.

The frequency was chosen with three frequency responses in mind: the transmitter, the receiving probe and the receiving amplifier. Also taken into consideration was the fact that the smallest dimension of the bar should be at least $5\lambda_r$ to insure propagation. Since the aluminum bar used for field pattern measurements has a surface wave velocity of about 9800 ft./sec. and a smallest dimension of 1 1/4 inches the frequency chosen must be greater than 470 kc. The frequency chosen was 760 kc. At this frequency the transmitter had a good impedance ratio, the probe was at its greatest sensitivity and the amplifier had ample gain.

The proper angle of incidence for the transmitter is 68° as given by equation (60). This was experimentally corroberated and the wedge was positioned 18 inches from the end of the bar.

Once the proper settings were achieved, care was exercised in maintaining them throughout the experiment. Before every test the pulse width, pulse amplitude, gate width and power supplies were checked. In the experiment a pulse width of 20 usec., a pulse amplitude of 35 volts peak-to-peak and a repetition rate of 500 pulse per second were used. The receiving gate width was set at 25 usec. to insure

that the entire wave pulse was recorded even if the gate was not positioned perfectly. This did not cause any trouble since at no time throughout the experiment did any other wave packet arrive at the probe at a time less than 5 usec. from the acoustic wave caused by the surface wave in the bar.

The transmitter, although designed to produce surface waves, also produced two other observable waves. One was a longitudinal wave in the bar and the second was a wave in the water due to the transmitter configuration. A shear wave in the bar was also produced, but since all observations were made in the liquid, this was not apparent. The problem now was to pick out that part of the wave in the water at the end of the bar produced by the surface wave. The technique used was that of timing the various wave packets. The time of arrival of each wave at the end of the bar could be predicted from the knowledge of the different wave velocities. Once the waves leave the end of the bar and go into the water they all travel with the same velocity and preserve their time separation. Since the longitudinal wave velocity in aluminum is 16,740 ft./sec. and the surface wave velocity in aluminum is 9,800 ft./sec., after a propagation distance of 18 inches the leading edges of these two wave pulses are 60 usec. apart. The water wave produced by the transducer, traveling at 5000 ft./sec., is now 210 usec. behind the body wave and 150 usec. behind the surface wave and was easily identified. Since the time separation between wave pulses at the end of the bar was at least 60 usec., a pulse width

of 20 usec. and a gate width of 25 usec. could be used. These predictions were shown to be correct by using the oscilloscope as a time measuring device and at the end of the bar all wave packets could be clearly distinguished.

The beam pattern measurements were taken by positioning the probe at a given height (relative to the top of the bar) and at a given distance from the end of the bar. The probe was then motor-driven along a path normal to the direction of wave propagation moving slowly enough so that the strength of one received pulse was not significantly different from the next to insure proper detecting and recording. In this manner, by changing the height and position of the probe and adjusting the gate to each new position, the acoustic field produced in the water by the surface wave in the bar was mapped.

VI. RESULTS

Experiments were conducted using 4 different bars. All the bars were of aluminum rolled stock and were the following sizes: 1" x 8" x 27" machined, 1 1/4" x 2" x 27" machined, 1 1/4" x 2" x 30" unfinished and 1/2" x 1" x 27" machined. See Figure 7 for a photograph of the bars. The smallest bar was used to investigate the question of medium thickness versus distance of surface wave propagation. The two bars with a 1 1/4" x 2" cross section were used to plot the beam pattern as well as to observe the effect of surface roughness on surface wave propagation. The largest bar was used to see what effect a large medium depth had on the beam pattern.

The pattern produced with the wedge 18 inches from the end of the 1 1/4" x 2" x 27" machined bar is shown in Figures 13, 14 and 15. Figures 13 and 14 show the pattern when the 1 1/4 inch dimension was used as the depth and Figure 15 shows the pattern when the 2 inch dimension was used as the depth. The surface wave launching technique used also produced a surface wave on the bottom of the bar of the same duration but of smaller amplitude. Since surface waves can travel around corners[13], the bottom surface wave would turn the corner, travel across the end of the bar, and interfere with the surface wave on top of the bar before the entire top wave packet had reached the end of the bar. For this reason the 2 inch dimension was then used as the depth

WEDGE 18" FROM END OF BAR
760 KC
BAR - ALUMINUM 1 1/4" x 2" x 27"

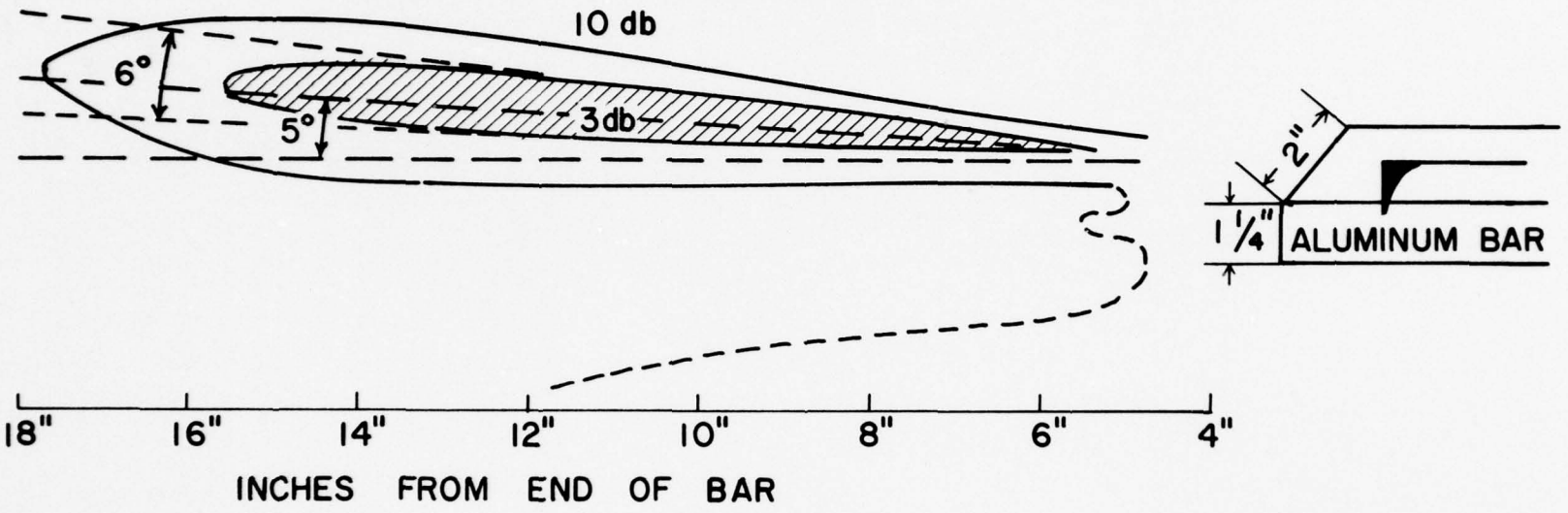

FIGURE 13 VERTICAL CROSS SECTION OF THE RADIATION PATTERN FROM A 1 1/4" THICK BAR

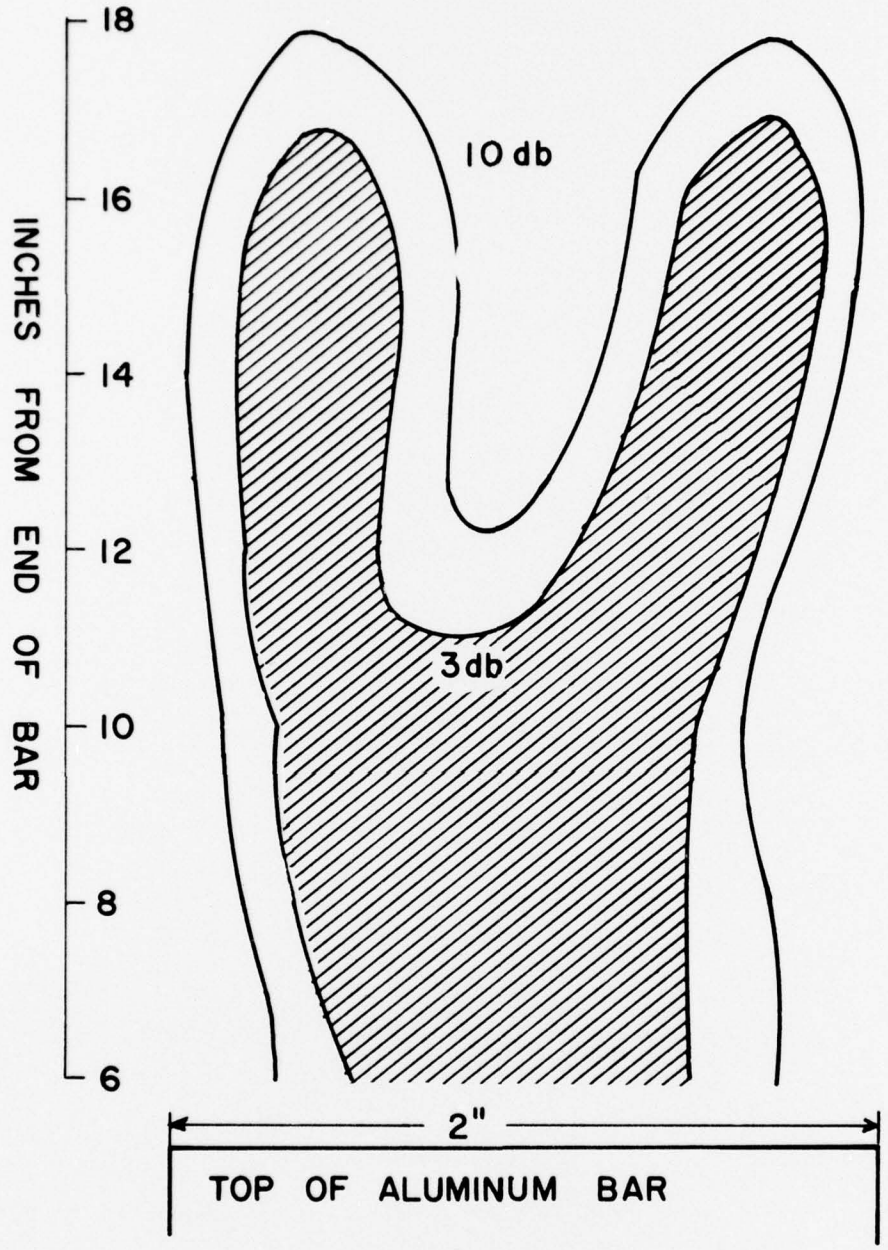

WEDGE 18" FROM END OF BAR
750 KC
BAR - ALUMINUM 1¼" × 2" × 27"

FIGURE 14 HORIZONTAL CROSS SECTION OF THE RADIATION PATTERN FROM A 2" WIDE BAR

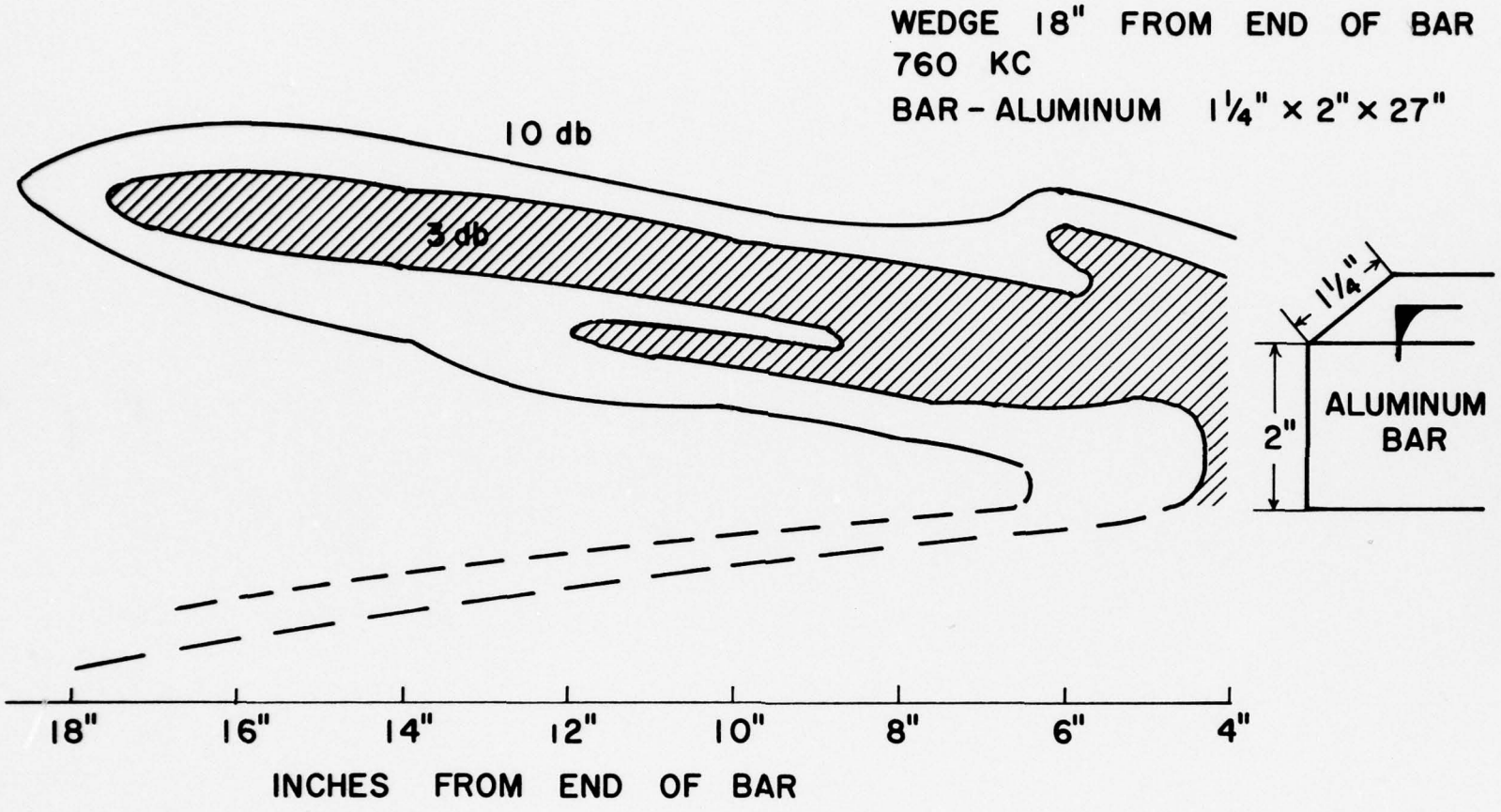

FIGURE 15 VERTICAL CROSS SECTION OF THE RADIATION PATTERN FROM A 2" THICK BAR

to avoid this interference resulting in the pattern shown in Figure 15. Due to the length of the tank, measurements at a distance greater than 20 inches from the end of the bar were unobtainable.

Field plots showed that a beam with a width approximately equal to the width of the bar is produced. This is expected since at a frequency of 760 kc the smallest dimension of the bar corresponds to $8\lambda_r$ while the 2 inch dimension corresponds to $13\lambda_r$ producing a long straight line source. The forked nature of this pattern as shown in Figure 14 most likely results from the surface wave energy being concentrated along the edges of the bar. The vertical cross section shown in Figure 13 with 3 db points only 6° apart is not so easily explained, nor is the angle at which the wave is propagated. Since almost all the energy of a surface wave is contained within one wavelength of the surface the resulting sharp pattern is surprising. The relatively small (5°) angle of the main lobe relative to the bar axis raises another question. The answer probably lies in the fact that with regard to equation (59) the third term on the right hand side causes the particle motion as shown in Figure 2 to be tilted with respect to the boundary. This tilt would then produce the observed angle of propagation.

The pencil like nature of the beam has two plausible causes. The first is that since there is also a surface wave on the bottom of the bar and these waves can propagate around corners, they may interfere with each other producing

the observed pattern. Secondly, the beam width may depend upon wedge distance from the end of the bar. Thus it may be possible to use the length of the radiator to match the bar to the fluid. In his paper "Surface Waves in Acoustics" Brekhovskikh[14] states that concerning the case of surface radiation from the end of a cylinder that by increasing the length of the radiator it is possible to make the width of the principle lobe of the directivity characteristic as small as we like.

A comparison of the two bars of the same dimensions, one being machined on all 6 faces and the other being used unfinished, showed no difference in the resulting pattern. However, the degree of attenuation of the surface wave with distance along the bar, although small in both cases, was greater in the unfinished bar. This was observed by probing along the surface of the bar as well as noting the difference in the strengths of the resulting fields.

The experiments with the smallest bar revealed that the thickness of the elastic solid is a definite factor in the distance of propagation. Using the 1/2" dimension as the depth, which corresponds to $3.3\lambda_r$, it was found that in a distance of 18 inches the surface wave had decreased to such an extent that only a very weak radiated pattern could be obtained. In the 18 inches of propagation its strenth had decreased to 1/10th of its original value and a scalloped pattern was produced due to the size of the bar compared to λ_r. The largest bar was also tried, but it was found that

although a similar pattern as shown in Figures 13, 14 and 15 existed, it was masked by the radiation produced by the surface wave traveling across the end of the bar.

VII. CONCLUSIONS

The conclusions of this investigation are:

1) A surface wave can be propagated along a boundary between an elastic solid and a liquid.
2) A pencil like beam pattern can be produced by this wave when launched from the end of a rectangular bar.
3) The surface condition of the bar is a factor in determining the decrease of surface wave energy with distance of propagation.
4) The distance of propagation of surface waves is a fuction of the thickness of the elastic solid.

There still remain many questions which warrant further study. These include the changes in beam pattern due to variations in radiator length, radiator dimensions relative to surface wave wavelength, and acoustic impedance (ρv) ratios of the solid and the liquid. Up to now many more questions have been raised than have been answered. Some further aspects of this work that should be looked into are:

1) Experimental investigation of the directivity versus radiator length by measuring the field with the wedge at different distances from the end of the bar.
2) An explination of how the surface wave propagates around a corner. How is the particle motion modified by the discontinuity in the elastic

medium? The answer to this could shed some light on the observed radiation directivity.

3) By use of some other suitable materials for the elastic solid, determine the effect of the acoustic impedance ratios on energy transmission into the fluid and beam angle of propagation.

BIBLIOGRAPHY

1. S. Timoshenko, Theory of Elasticity, Mc Graw Hill, 1934

2. Robert Bruce Lindsay, Mechanical Radiation, Mc Graw Hill, 1960.

3. Lord Rayleigh, "On Waves Propagated Along the Plane Surface of an Elastic Solid", Proceedings of the London Mathematical Society, Vol. 17 pp. 4-11, 1885

4. Sir Harold Jeffreys, The Earth, Cambridge University Press, 1959.

5. E. G. Cook and H. E. Van Valkenberg, "Surface Waves at Ultrasonic Frequencies", ASTM Bulletin, May 1954

6. I. G. I. Scholte, "Rayleigh Waves in Isotropic and Anisotropic Media",Meded. en Verhandel. Koninkl. nederl. Meterlogical Institute, 72 pp.44, 1958

7. I. A. Viktorov and R. A. Grigoryan, "Quasi-Rayleigh Waves in an Elastic Layer", Soviet Physics-Acoustics Vol. 5 No. 3 pp.373-375, February 1960

8. N. C. Yen and F. H. Middleton, "Model Experiments on Underwater Sound Reflection From a Corrugated Boundary", Tech. Report No. 1, U. S. Navy Underwater Ordinance Station Newport, R. I., October 1961

9. C. Minton, "Inspection of Metals with Ultrasonic Waves", Non Destructing Testing Vol. 12 No. 4 pp.13-16, 1954

10. M. Auberger and J. S. Rinehart, "Ultrasonic Attenuation of Longitudinal Waves in Plastics", Journal of Applied Physics Vol. 32 No. 2 pp.219-222, February 1961

11. K. N. Vinogradov and G. K. Ul'yanov, "Measurements of the Velocity and Attenuation of Ultrasonic Surface Waves in Hard Materials", Soviet Physics-Acoustics Vol. 5 No.3 pp.296-299, February 1960

12. I. A. Viktorov, "Investigation of Methods for Exciting Rayleigh Waves", Soviet Physics-Acoustics Vol. 7 No. 3 January-March 1962

13. I. A. Viktorov,"Rayleigh Waves in the Ultrasonic Range", Soviet Physics-Acoustics Vol. 8 No. 2,Oct.-Dec. 1962

14. L. M. Brekhovskikh, "Surface Waves in Acoustics", Soviet Physics-Acoustics Vol. 5 No. 1 , January-March 1959

APPENDIX A

Obtaining Stress In Terms Of Strain

Using Hooke's law stresses can be written in terms of strains as follows:

$$\epsilon_x = \frac{1}{E}\left[\sigma_x - \nu(\sigma_y+\sigma_z)\right] \text{ or } E\epsilon_x = \sigma_x - \nu\sigma_y - \nu\sigma_z \qquad \text{(A-1)}$$

$$\epsilon_y = \frac{1}{E}\left[\sigma_y - \nu(\sigma_x+\sigma_z)\right] \text{ or } E\epsilon_y = -\nu\sigma_x + \sigma_y - \nu\sigma_z \qquad \text{(A-2)}$$

$$\epsilon_z = \frac{1}{E}\left[\sigma_z - \nu(\sigma_x+\sigma_y)\right] \text{ or } E\epsilon_z = -\nu\sigma_x - \nu\sigma_y + \sigma_z \qquad \text{(A-3)}$$

Solving for σ_x

$$\sigma_x = \frac{\begin{vmatrix} E\epsilon_x & -\nu & -\nu \\ E\epsilon_y & 1 & -\nu \\ E\epsilon_z & -\nu & 1 \end{vmatrix}}{\begin{vmatrix} 1 & -\nu & -\nu \\ -\nu & 1 & -\nu \\ -\nu & -\nu & 1 \end{vmatrix}} = \frac{E\epsilon_x + \nu^2 E\epsilon_y + \nu^2 E\epsilon_z + \nu E\epsilon_z + \nu E\epsilon_y - \nu^2 E\epsilon_x}{1 - \nu^3 - \nu^3 - \nu^2 - \nu^2}$$

$$\sigma_x = \frac{E\left[\epsilon_x(1-\nu^2) + \epsilon_y(\nu+\nu^2) + \epsilon_z(\nu+\nu^2)\right]}{-2\nu^3 - 3\nu^2 + 1}$$

$$\sigma_x = \frac{E\left[\epsilon_x(1-\nu^2) + \nu(1+\nu)\epsilon_y + \epsilon_z\right]}{(\nu+1)(\nu+1)(-2\nu+1)} \qquad \text{(A-4)}$$

now $(1-\nu^2) = (1+\nu)(1-2\nu) + \nu(1+\nu)$. Therefore

$$\sigma_x = \frac{E\left[\left\{(1+\nu)(1-2\nu) + \nu(1+\nu)\right\}\epsilon_x + \nu(1+\nu)(\epsilon_y+\epsilon_z)\right]}{(\nu+1)(\nu+1)(1-2\nu)}$$

$$= E\left[\frac{\epsilon_x}{(\nu+1)} + \frac{\nu(\epsilon_x+\epsilon_y+\epsilon_z)}{(\nu+1)(1-2\nu)}\right. \tag{A-5}$$

$$\sigma_x = \frac{\nu E_f}{(\nu+1)(1-2\nu)} + \frac{E\epsilon_x}{\nu+1} \tag{A-6}$$

Similarly $$\sigma_y = \frac{\nu E_f}{(\nu+1)(1-2\nu)} + \frac{E\epsilon_y}{\nu+1} \tag{A-7}$$

$$\sigma_z = \frac{\nu E_f}{(\nu+1)(1-2\nu)} + \frac{E\epsilon_z}{\nu+1} \tag{A-8}$$

APPENDIX B

Displacement Directions Of Longitudinal and Transverse Waves

With reference to equations (18) and (19), the direction of particle displacement can be found for both longitudinal and transverse waves.

a) Longitudinal[2]

$$V_L = \sqrt{\frac{\lambda+2G}{\rho}} \tag{B-1}$$

which means that u, v, w are propagated with the same velocity (irrotational). Assume u, v, w are functions of x and t only and do not depend upon y and z. Equation (B-1) then reduces to the three equations

$$\ddot{u} = \frac{V^2\partial^2 u}{\partial x^2}\ , \quad \ddot{v} = \frac{V^2\partial^2 v}{\partial x^2}\ , \quad \ddot{w} = \frac{V^2\partial^2 w}{\partial x^2} \tag{B-2}$$

now since $\vec{A}$ is irrotational $\nabla x\vec{A}=0$ and

$$\frac{\partial w}{\partial y} = \frac{\partial v}{\partial z} \qquad \frac{\partial u}{\partial z} = \frac{\partial w}{\partial x} \qquad \frac{\partial v}{\partial x} = \frac{\partial u}{\partial y}$$

but since u, v, and w are functions of x and t only

$\frac{\partial v}{\partial x} = \frac{\partial w}{\partial x} = \frac{\partial u}{\partial y} = \frac{\partial u}{\partial z} = 0$ and hence v is not a function of x and u is a function of x only.

Therefore, the only propagated displacement is u, which is directed along the direction of propagation.

b) Transverse[2]

$$V_S = \sqrt{G/\rho} \qquad (B\text{-}3)$$

Assuming as above that $\vec{A}$ depends on x and t alone and since now $\vec{A}$ is solenoidal($\nabla \cdot \vec{A} = 0$) we readily see that here $\frac{\partial u}{\partial x} = 0$ and hence u is not propagated as a wave. This means that the propagated displacement is perpendicular to the direction of propagation.

APPENDIX C

Evaluation Of A(z) and B(z)

In order to find the exact form of the velocity potentials ϕ and Ψ we must determine A(z) and B(z).

Substituting Equation (23) into Equation (13) with no body forces

$$\rho \frac{d^2}{dt^2}\left(\frac{\partial \phi}{\partial x} + \frac{\partial \Psi}{\partial z}\right) = (\lambda+G)\frac{\partial \Gamma}{\partial x} + G\nabla^2\left(\frac{\partial \phi}{\partial x} + \frac{\partial \Psi}{\partial z}\right) \tag{C-1}$$

now

$$\frac{\partial \Gamma}{\partial x} = \frac{\partial}{\partial x}\left(\frac{\partial u}{\partial x} + \frac{\partial v}{\partial y} + \frac{\partial w}{\partial z}\right) = \frac{\partial^2 u}{\partial x^2} + \frac{\partial^2 v}{\partial x \partial y} + \frac{\partial^2 w}{\partial x \partial z}$$

$$= \frac{\partial^2}{\partial x^2}\left(\frac{\partial \phi}{\partial x} + \frac{\partial \Psi}{\partial z}\right) + 0 + \frac{\partial^2}{\partial x \partial z}\left(\frac{\partial \phi}{\partial z} - \frac{\partial \Psi}{\partial x}\right)$$

$$= \frac{\partial}{\partial x}\left(\frac{\partial^2 \phi}{\partial x^2} + \frac{\partial^2 \Psi}{\partial x \partial z} + \frac{\partial^2 \phi}{\partial z^2} - \frac{\partial^2 \Psi}{\partial x \partial z}\right) \tag{C-2}$$

$$\therefore \frac{\partial \Gamma}{\partial x} = \nabla^2 \phi \tag{C-3}$$

Separating ϕ in Ψ in (C-1)

$$\rho \frac{d^2}{dt^2}\frac{\partial \phi}{\partial x} = (\lambda+G)\frac{\partial}{\partial x}\nabla^2\phi + G\nabla^2\left(\frac{\partial \phi}{\partial x}\right) \tag{C-4}$$

$$\rho \frac{d^2 \phi}{dt^2} = (\lambda+G)\nabla^2\phi + G\nabla^2\phi = (\lambda+2G)\nabla^2\phi \tag{C-5}$$

and

$$\rho \frac{d^2}{dt^2}\left(\frac{\partial \Psi}{\partial z}\right) = G\nabla^2\left(\frac{\partial \psi}{\partial z}\right)$$

$$\rho \frac{\partial^2 \psi}{\partial t^2} = G\nabla^2 \psi \qquad \text{(C-6)}$$

Substituting (26 A) into (C-6)

$$\rho \frac{\partial^2 \phi}{\partial t^2} = -\rho k^2 c^2 A(z) \exp ik(x-ct) = (\lambda+G)\left(\frac{d^2 A(z)}{dz^2} - A(z)k^2\right)\exp ik(x-ct)$$

$$-k^2 c^2 A(z) = \alpha^2\left(\frac{d^2 A(z)}{dz^2} - k^2 A(z)\right) \qquad \text{(C-7)}$$

where $\alpha = \sqrt{\frac{\lambda+2G}{\rho}} = V_L$

$$A(z) = C \exp[-rz] \qquad \text{(C-8)}$$

where C is a constant.

Now substituting (26 B) into (C-6)

$$\rho \frac{\partial^2 \psi}{\partial t^2} = -\rho k^2 c^2 B(z) \exp ik(x-ct) = G\left(-k^2 B(z) + \frac{\partial^2 B(z)}{\partial z^2}\right)\exp ik(x-ct)$$

$$-k^2 c^2 B(z) = \beta^2\left(\frac{d^2 B(z)}{dz^2} - k^2 B(z)\right) \qquad \text{(C-9)}$$

$$\therefore B(z) = D \exp[-sz] \qquad \text{(C-10)}$$

where $\beta = V_T = \sqrt{G/\rho}$ and $D = \frac{2ikrC}{s^2+k^2}$ (C-11)

Substituting (C-8) into (C-7) yields

$$-k^2c^2C \exp[-rz] = \alpha^2(r^2C \exp[-rz] - k^2C \exp[-rz])$$

$$\therefore \frac{r^2}{k^2} = 1 - c^2/\alpha^2 \qquad (27A)$$

and substituting (C-10) into (C-9) yields

$$-k^2c^2D \exp[-sz] = \beta^2(s^2D \exp[-sz] - k^2D \exp[-sz])$$

$$\therefore \frac{s^2}{k^2} = 1 - c^2/\beta^2 \qquad (27B)$$

APPENDIX D

Derivation Of The Rayleigh Wave Equation

Knowing the boundary conditions, the velocities of the longitudinal and transverse waves and the displacements in terms of the velocity potentials the Rayleigh wave equation can be derived.

The velocity equations can be written as

$$\lambda + 2G = \rho\alpha^2, \quad G = \rho\beta^2 \tag{D-1}$$

Using equation (C-11) which is $D = \frac{2ikrC}{s^2+k^2}$ (D-2)

and substituting it into equation (32) yields

$$-\lambda k^2 C + (\lambda+2G) r^2 C + \frac{4i^2 k^2 rsC}{s^2+k^2} = 0$$

or

$$-\frac{\lambda}{G} + \left(\frac{\lambda+2G}{G}\right)\frac{r^2}{k^2} - \frac{4rs}{s^2+k^2} = 0 \tag{D-3}$$

From (D-1) $\lambda = \rho\alpha^2 - 2G$

$$\therefore \frac{\lambda}{G} = \frac{\rho}{G}\alpha^2 - 2 = \frac{\alpha^2}{\beta^2} - 2 \tag{D-4}$$

and

$$\frac{\lambda+2G}{G} = \frac{\alpha^2}{\beta^2} \tag{D-5}$$

Using the compatibility equations (27) and substituting (D-4) and (D-5) into (D-3) yields

$$2 - \frac{c^2}{\beta^2} = \frac{4rs}{s^2+k^2} \qquad \text{(D-6)}$$

Squaring both sides and using equation (27) for r^2 and s^2 yields

$$\left(2 - \frac{c^2}{\beta^2}\right)^2 = \frac{16k^4(1-c^2/\alpha^2)(1-c^2/\beta^2)}{k^4(4-4c^2/\beta^2 + c^4/\beta^4)} = \frac{16(1-c^2/\alpha^2)(1-c^2/\beta^2)}{(2-c^2/\beta^2)^2}$$

$$\left(2 - \frac{c^2}{\beta^2}\right)^4 = 16(1-c^2/\beta^2)(1-c^2/\beta^2) \qquad \text{(D-7)}$$

Expanding both sides and setting the right hand side equal to zero results in the Rayleigh wave equation which is

$$\frac{c^2}{\beta^2}\left[\frac{c^6}{\beta^6} - 8\,\frac{c^4}{\beta^4} + \frac{c^2}{\beta^2}\left(24 - 16\,\frac{\beta^2}{\alpha^2}\right) - 16\left(1 - \frac{\beta^2}{\alpha^2}\right)\right] = 0 \qquad (33)$$